

2017-01-01

# Design and Development of a Foil Application Tool for a Foil Embedding Process in the Multi3D Manufacturing System

Betty Elizabeth Mckenzie

University of Texas at El Paso, bemckenzie@miners.utep.edu

Follow this and additional works at: [https://digitalcommons.utep.edu/open\\_etd](https://digitalcommons.utep.edu/open_etd)



Part of the [Mechanical Engineering Commons](#)

---

## Recommended Citation

Mckenzie, Betty Elizabeth, "Design and Development of a Foil Application Tool for a Foil Embedding Process in the Multi3D Manufacturing System" (2017). *Open Access Theses & Dissertations*. 696.  
[https://digitalcommons.utep.edu/open\\_etd/696](https://digitalcommons.utep.edu/open_etd/696)

This is brought to you for free and open access by DigitalCommons@UTEP. It has been accepted for inclusion in Open Access Theses & Dissertations by an authorized administrator of DigitalCommons@UTEP. For more information, please contact [lweber@utep.edu](mailto:lweber@utep.edu).

DESIGN AND DEVELOPMENT OF A FOIL APPLICATION TOOL FOR A FOIL  
EMBEDDING PROCESS IN THE MULTI<sup>3D</sup> MANUFACTURING SYSTEM

BETTY ELIZABETH McKENZIE

Master's Program in Mechanical Engineering

APPROVED:

---

Ryan Wicker, Ph.D., Chair

---

Norman Love, Ph.D.

---

David Roberson, Ph.D.

---

Charles Ambler, Ph.D.  
Dean of Graduate School

Copyright ©

By

Betty Elizabeth McKenzie

2017

## **DEDICATION**

This Thesis is dedicated to My Loving and Supportive Family. They are a Team that is Always Rooting for Me and I Could Not Imagine Having a More Loyal and Loving Support System. My Success and Accomplishments Could Not Have Been Possible Without Them. Thank You.

DESIGN AND DEVELOPMENT OF A FOIL APPLICATION TOOL FOR A FOIL  
EMBEDDING PROCESS IN THE MULTI<sup>3D</sup> MANUFACTURING SYSTEM

by

BETTY ELIZABETH McKENZIE B.S. in Mechanical Engineering

THESIS

Presented to the Faculty of the Graduate School of  
The University of Texas at El Paso  
in Partial Fulfillment  
of the Requirements  
for the Degree of

MASTER OF SCIENCE

Department of Mechanical Engineering

THE UNIVERSITY OF TEXAS AT EL PASO

May 2017

## ACKNOWLEDGMENTS

I would like to acknowledge Dr. Ryan Wicker, director of the W.M. Keck Center for 3D Innovation (Keck Center), for his support in my research as an undergraduate and graduate student. Mr. David Espalin, associate director of the Keck Center, is an invaluable mentor who has guided me throughout my work to become a better engineer. These two individuals have created a space here at the Keck Center where new ideas are inspired and strong work ethics are developed. I would also like to thank America Makes, the National Additive Manufacturing Innovation Institute for providing funding. A special thank you to my committee members Dr. Norman Love and Dr. David Roberson for their guidance in reviewing this thesis and being a part of a special accomplishment.

Many other people in the Keck Center also deserve recognition. Mr. Christopher Minjares for machining and help in constructing many of the components to the project described below. Ms. Lluvia Herrera and Mr. Jaime Varela for their help in the development of the automated syringe pump for dispensing the adhesive. I would also like to thank Mr. Jose Coronel and Mr. Steven Ambriz for their help in the design of the substrate and the use of the equipment in the testing procedures, also Mr. Daniel Marquez for his input in the mounting of the tool; and thank you to Mr. Jose Motta for assisting with all of the electrical components in the project.

I would like to acknowledge those who have supported me and encouraged my continued education, my family. My parents Elizabeth McKenzie and Michael McKenzie Sr., my sister Hazel McKenzie, and my brothers James McKenzie and Michael McKenzie Jr. whom have

always been there in a loving and supportive way. Most importantly I thank God for the blessings he has bestowed upon me.

## **ABSTRACT**

Additive manufacturing (AM) encompasses different technologies, including material extrusion 3D printing, a technology commonly referred to as fused deposition modeling (FDM), which is the focus of the work described in this manuscript. Additive manufacturing is a growing technology with many applications in numerous fields from the air force to medical offices. FDM is a process that uses thermoplastics, in this case polycarbonate (PC), where the PC is heated and selectively dispensed in a layer-by-layer process to create a 3D printed part. Currently, FDM systems have advantages over subtractive manufacturing or machining because cavities and other components (e.g., microchips, valves, and actuators) can be inserted at any layer. However, the FDM systems are limited in the functionality and purposes of the end-use product. Limited by the ability of printing one nonconductive material at a time, the commercially available FDM system cannot create parts with electrical functionality. Incorporating multiple materials such as the addition of conductive copper with the printed PC can mitigate the limitations of a conventional 3D printed part. Incorporation of conductive materials can create features such as electrically conductive traces, thermally dissipating heatsinks, and electromagnetic radiating elements. While there are efforts to fully automate the fabrication of electronic devices within the arena of 3D printing, the addition of electrical components into 3D printed parts is most commonly done by hand. There is a need to incorporate electrical components into parts using an automated method. The same is true when referring to placing and patterning conductive foils within 3D printed parts. Thus, the goal of this work is to develop a tool that will enable foil application within 3D printed parts.

For this work, a Stratasys Fortus 400mc FDM machine was used to fabricate PC parts. A hybrid manufacturing (HM) process was used, which can be described as an approach to



building a product with additive and subtractive manufacturing. There are many ways to create a HM process, depending on the desired end result various manufacturing applications could be turned into a HM process. This work describes the design and development of a Foil Application (FA) tool for foil embedding into 3D printed parts to result in a HM process. With the use of a 3D printer and milling machine a HM process was created.

The FA tool was designed and implemented as an automated tool for applying copper foil onto the surface of a printed substrate. The copper foil was then machined using the CNC to create patterns. Copper foils were patterned for dissipating heat, but other potential patterns include circuits, ground planes or an electrical connection between layers, just to name a few. The FA tool included the capabilities of varying the feed rate of the dispensed copper foil, handling different copper gauge thicknesses and widths not to exceed 25.4 mm (1 inch). The ultimate goal of these efforts was to incorporate the FA tool into the Multi<sup>3D</sup> Manufacturing System where a new generation of HM processes would be executed by one machine. The results of these new HM processes will ultimately culminate in the fabrication of complex parts with electrical capabilities through the embedding of copper foil. In previous work, electronic components in a 3D printed part were manually added after pausing and removing the substrate from the printer. The manual intervention proved to introduce registration errors and was deemed to be labor-intensive and tedious. The goal of the FA tool was to create a HM system that would eliminate human interaction in the building process; therefore creating a fully automated system to mitigate registration errors and tedious operations. The result would be a completed complex print with electronic capabilities with the unique capabilities of a 3D printer.

Upon completion of the FA tool, experiments were done; those of which resulted in multiple findings. First, the FA tool applied the foil to a designated position within 8% of the

specified location. Also, the addition of embedded foil decreased the flexural extension of the PC part with the increase of width of the foil. With the addition of 12.7 mm copper foil the percent decrease of the flexural extension compared to the samples without foil was 19% and 42% for the 25.4 mm foil. Tests were done to determine how straight a copper strip could be applied along a 76.2 mm (3 inches) length. The length was user-designated and was not chosen for specific reasons. It was important to test how straight the copper foil strip was applied because different applications of the copper foil could require straight strips. Foil applications such as ground planes for antennas require specific location and dimensions of the copper for accuracy on electromagnetic response data. The copper showed a maximum horizontal displacement of 0.4 mm on either side along its length of 76.2 mm. Lastly, one, two and three copper foil strips were applied to three separate parts along three faces of a PC block. One of the exposed sides of the copper was positioned onto a heating plate. Thermocouples were evenly placed across three faces of the part to determine the temperature distribution across the PC part. There was a decrease of change in temperature across the copper foil with an increase of copper foil surface area. The percent difference between the part with no foil and one foil strip was a 26.3 percent increase. The percent increase from one foil to three foils was 37.5%.

These findings showed that the addition of a copper foil application tool was beneficial since applying copper foils aided in the temperature distribution of a heated PC part. The potential to integrate this tool into a single Multi<sup>3D</sup> machine would ultimately provide time-savings. The foil application process before the FA tool required the removal of the build platform, cool down time, manual application of the foil, and reheat time after the build platform was placed back into the printer. With the incorporation of the FA tool, these steps can be eliminated. With the tool inside the printer, the build platform would remain inside the printer

and the cool down and heating time would be eliminated, making the multi-material integration faster than if done by hand. Not only would the incorporation of the tool into the printer speed up the application process but it would reduce the registration errors. When the substrate is removed from the printer and cools down, the part contracts. When the platform is returned to the printer and begins to reheat again, the substrate does not fully expand again; resulting in subsequent layers not lining up when deposited, creating a registration error.

Two different adhesive methods were developed and demonstrated in context of the PC and copper adhesion. One side was adhered to a cooler (147°C), solid PC surface; the other was exposed to a dispensed, semi-solid, hot (365°C) amorphous thermoplastic. The pre process required an adhesive and associated accelerant to adhere the solid PC substrate with the applied copper foil. The accelerant reduced the adhesion time, from 30 seconds to under ten seconds to adhere as the tool applied the copper foil. Subsequent layers of semi-solid PC were printed over the applied copper foil without post processing chemicals, the result of which was a rough textured surface finish with exposed copper foil in some places. Three chemicals were added to adhere the copper foil with the top layer of PC. The first was etchant: a chemical that etched the surface of the copper and removed the protective oxide layer. Then Isopropyl alcohol was added to remove excess etchant and clean the surface of the foil. Lastly an Acrylonitrile Butadiene Styrene (ABS) and acetone solution was added. The ABS solution was a thick liquid used to adhere the copper foil with the subsequently printed materials.

At the conclusion of the testing of the FA tool, the produced results exhibited that the FA tool could apply copper foil under a ten percent error. Electronic components, structural purposes and thermal dissipation are all within the capabilities of the FA tool in the Multi<sup>3D</sup>

Manufacturing System. Foil embedding through the application of foil application with the FA tool has proven to be an automated process with multiple purposes.

## TABLE OF CONTENTS

ACKNOWLEDGEMENTS.....	v
ABSTRACT.....	vii
TABLE OF CONTENTS.....	xii
LIST OF TABLES.....	xiv
LIST OF FIGURES.....	xv
Chapter 1. INTRODUCTION.....	1
1.1 Background.....	1
1.2 Motivation.....	3
1.3 Thesis Objective.....	5
1.4 Thesis Outline.....	5
Chapter 2. LITERATURE REVIEW.....	6
2.1 Introduction.....	6
2.2 The Seven Process Categories of Additive Manufacturing.....	6
2.3 Embedded Electronic Components in 3D Printing.....	9
Chapter 3. FOIL APPLICATION TOOL.....	13
3.1 Concept.....	13
3.2 Design Objectives.....	13
3.3 Design Constraints.....	14

3.4 Iteration of Design.....	15
3.5 Material and Component Selection.....	23
3.6 Application and Embedding Process.....	27
Chapter 4. DESIGN EVALUATION/EXPERIMENTATION.....	33
4.1 Demonstration: CNC End Mill Cut Out of Patterns.....	33
4.2 Testing.....	34
4.3 Results.....	40
Chapter 5. CONCLUSION AND FUTURE WORK.....	60
5.1 Conclusion.....	60
5.2 Future Work.....	62
REFERENCES.....	64
APPENDIX.....	68
CURRICULUM VITA.....	78

## LIST OF TABLES

<b>Table 4.1</b> Foil 4 averages for all five slices.....	55
---	----

## LIST OF FIGURES

<b>Figure 1.</b> 2015 unit sales market share estimates among manufacturers of industrial AM systems worldwide (image courtesy of Caffery et al., 2016).....	8
<b>Figure 2.</b> A) First manufactured design of the FA Tool, B) iterated design of the FA Tool.....	15
<b>Figure 3.</b> Roller sub assembly.....	17
<b>Figure 4.</b> Roller with excess adhesive after application.....	18
<b>Figure 5.</b> A) TSINY Gear Box Motor with a lower torque, B) final motor with a higher torque.....	19
<b>Figure 6.</b> A) Guide with spacer, B) crooked applied foil.....	20
<b>Figure 7.</b> Side view of the spring loaded roller.....	21
<b>Figure 8.</b> Design two of the FA Tool applying copper foil onto a substrate.....	22
<b>Figure 9.</b> Initial testing of adhesive with accelerant.....	26
<b>Figure 10.</b> FA Tool with labeled axes.....	28
<b>Figure 11.</b> Multi <sup>3D</sup> Manufacturing System (Ambriz, 2015).....	29
<b>Figure 12.</b> A) Left sample of foil after being applied with accelerant, B) right sample of foil after being applied with accelerant.....	30
<b>Figure 13.</b> A) FA Tool applying copper foil, B) applied foil after FA Tool was removed, C) excess material was removed, D) etchant was applied to copper foil, E) isopropanol added after etchant.....	31



<b>Figure 14.</b> A) Black ABS Solution, B) resulting part, C) white ABS Solution, D) resulting part.....	32
<b>Figure 15.</b> A) Printed substrate with indentions, B) post application, C) CNC Router cutting out preprogrammed shapes, D) resulting applied copper foil.....	33
<b>Figure 16.</b> A) Full width copper foil strip applied and printed over without post process chemicals, B) cut out of circular patterns and printed over without post process chemicals.....	34
<b>Figure 17.</b> Applying copper foil to heat transfer part.....	37
<b>Figure 18.</b> Thermocouples attached to heat transfer part.....	38
<b>Figure 19.</b> Testing apparatus, A) DAQ system, B) thermal paste, C) heat transfer part, D) heating plate.....	39
<b>Figure 20.</b> Heat transfer part placed onto heating plate.....	40
<b>Figure 21.</b> Flexural specimens posttest (no foil), A) sample 1, B) sample 2, C) sample 3.....	41
<b>Figure 22.</b> Stress Strain graph of no foil specimen for three treatments.....	42
<b>Figure 23.</b> Flexural specimens posttest (12.7 mm foil), A) sample 1, B) sample 2 arrow indicates location of fracture, C) sample 3.....	44
<b>Figure 24.</b> Stress Strain Graph of 12.7 mm foil specimen for three treatments.....	44
<b>Figure 25.</b> Flexural specimens posttest (25.4 mm foil), A) sample 4, B) sample 5, C) sample 6.....	46
<b>Figure 26.</b> Stress Strain graph of 25.4 mm foil specimen for three treatments.....	46
<b>Figure 27. Maximum</b> Flexural Stress graph of three treatments.....	47

<b>Figure 28.</b> Flexural Extension graph of three treatments.....	49
<b>Figure 29.</b> Test of straightness specimens A) part 1 arrow indicates wrinkle of foil, B) part 2, C) part 3, D) part 4, E) part 5.....	50
<b>Figure 30.</b> Graph of change in distance from foil to the edge of substrate (Part 1).....	51
<b>Figure 31.</b> Straightness test box plot for measurements from edge of five specimens.....	52
<b>Figure 32.</b> Slice 4 of the four layer embedded sample.....	53
<b>Figure 33.</b> Graph of slice 4 of the four layer embedded sample, hollow circles indicate expected values, and solid circles indicate actual values (the numbering of each series as per the next example).....	54
<b>Figure 34.</b> Warped test substrate.....	55
<b>Figure 35.</b> Graph of heat transfer at measurement 1 (note that the series No Foil, One Foil and Two Foils were similar and as such the Two Foils series was unobservable in the chart).....	56
<b>Figure 36.</b> Graph of heat transfer at measurement 5.....	57
<b>Figure 37.</b> Graph of the change in temperature across one foil vs. the change in surface area...58	
<b>Figure 38.</b> First design of FA Tool.....	68
<b>Figure 39.</b> A) Etchant, B) accelerant, C) adhesive.....	68
<b>Figure 40.</b> Sample 5 of flexural testing in the Instron.....	69
<b>Figure 41.</b> Graph of change in distance from foil to the edge of substrate (Part 2).....	70
<b>Figure 42.</b> Graph of change in distance from foil to the edge of substrate (Part 3).....	70

<b>Figure 43.</b> Graph of change in distance from foil to the edge of substrate (Part 4).....	71
<b>Figure 44.</b> Graph of change in distance from foil to the edge of substrate (Part 5).....	71
<b>Figure 45.</b> OGP measuring slice 5 of the four layer embedded sample.....	72
<b>Figure 46.</b> Graph of slice 1 of the four layer embedded sample.....	72
<b>Figure 47.</b> Graph of slice 2 of the four layer embedded sample.....	73
<b>Figure 48.</b> Graph of slice 3 of the four layer embedded sample.....	73
<b>Figure 49.</b> Graph of slice 5 of the four layer embedded sample.....	74
<b>Figure 50.</b> Sketch of heat transfer part with dimensions.....	74
<b>Figure 51.</b> Thermal paste.....	75
<b>Figure 52.</b> Computer generated graph from data collected through the DAQ system.....	75
<b>Figure 53.</b> Graph of heat transfer at measurement 2.....	76
<b>Figure 54.</b> Graph of heat transfer at measurement 3.....	76
<b>Figure 55.</b> Graph of heat transfer at measurement 4.....	77

## **CHAPTER 1**

### **INTRODUCTION**

#### **1.1 Background**

In the late 1980's, additive manufacturing (AM) technologies included machines that could create similar products to those designed on computer software, with the ability to use them as models for physical representations. In the time since then, AM processes have developed. Companies and labs such as the W. M. Keck Center for 3D Innovation at the University of Texas at El Paso are now developing avant-garde printers and products. Carbon 3D, a company in Redwood City, California that uses the vat photo polymerization process was in the top ten fastest printers on the market in 2014 (Sher, 2016). The Carbon 3D printer prints roughly 25 times faster than stereolithography (SL) printers. The world of 3D printing has changed so much; printed models do not only represent prototypes of a design, but are now the product themselves with the capabilities of creating moving parts and interlayer embedding that would otherwise be impossible with subtractive manufacturing or other manufacturing applications such as resin casting or compression molding.

The fused deposition modeling (FDM) technology developed and trademarked by Stratasys Inc., is an AM process categorized as material extrusion. FDM uses thermoplastic material such as Nylon 12, ULTEM 9085 and 1010, and PC. Amorphous thermoplastics maintain a flow able state when the temperature is above the glass transition temperature. The thermoplastic will re-harden when the temperature lowers below the glass transition temperature. Creating a solid 3D printed model at the completion of the print.

The foil application (FA) tool is a way to semi-automate the process of applying embedded copper foil onto a 3D printed substrate. The layer by layer process of printing thermoplastics allows for the insertion of components such as the copper foil to create a multipurpose product. It is important to note that the applications for the embedded copper foil with the FA tool are for either electrical or heat transfer purposes in the testing done for this thesis. The thermoplastics used in the experiments were electrically nonconductive and had a low thermal conductivity. To compare, PC's thermal conductivity is  $0.22 \frac{W}{m K}$  and the thermal conductivity of Aluminum 6061 is  $173 \frac{W}{m K}$ .

The process of creating a FDM printed part is as follows. Before printing, a software-based 3D model needs to be generated. There are two ways in which to create this 3D model; the first and most common is drawing a solid model in computer-aided design (CAD) software. The other is by scanning an existing and probably more intricate object, such as a coral reef or a human organ. When the 3D model is complete, the file is saved as a STL file to open in Insight. Insight is a program proprietary to Stratasys that creates the machine instructions for the printer. In Insight, the orientation of the build is chosen and the model and support materials needed to create the part are determined by slicing each layer and creating the toolpaths. At this stage in the printing process, machine pauses can be programmatically added at specified layers. Selecting the layer(s) to pause will stop the printer from completing the print at those layers until the print is manually resumed. The new file created in Insight is saved as a CMB file. The CMB file can then be opened in Control Center, the final software to send the print. Here the 2D outline of the top view of the part is visible. The software allows for the user to determine the placement of the model on the build platform in the printer. After the printer is selected, the file

is sent to be printed. The user confirms the print on the printer's human machine interface and the layer-by-layer process begins extruding both support and model material.

The FDM technology consists of using a heated envelope and a heated extrusion tip to extrude the material. The heated extrusion tip contains a solid printing material fed through the printer. The material is heated to a flow able state before being extruded onto the platform. The heated extrusion tip and the heated envelope work hand in hand to create a printed part. The heated envelope maintains a consistent temperature. The purpose being is to maintain a temperature that will prevent the subsequently printed material from contracting due to the temperature difference after the material has already been dispensed. If the envelope was not heated, the new layers being printed would be warmer than the lower layers already dispensed. Beginning to cool and contract, the bond between layers would result in a registration error (an offset between layers). Therefore the heated envelope maintains a consistent temperature, limiting contraction (shrinkage) in previous and subsequent layers. This same registration error occurs when the print is paused at a layer, (a printer such as the Fortus 400mc can pause mid-print) and removed from the printing envelope for various processing reasons and then placed back into the printer to resume the print. While outside of the heated envelope the test piece cools causing it to contract. When placed back into the printer it does not fully expand again. When the print is complete the post processing will either require a manual removal of the support material or an ultrasonic bath to remove the harder to remove support material.

## **1.2 Motivation**

The most common type of 3D printing machine in the market today is a single model material extruder that can be paused between layers (Yusuf, 2016). The interruption between

layers offers the opportunity to manually insert objects such as magnets and/or coils to create a motor. The print can then be resumed and the additional inserted objects within the print will be encapsulated. However, to accomplish this task the print needs to be paused adding additional labor time and human interaction. If the printer includes a heated envelope, the object being printed will likely need to be removed from the heated envelope of the printer for the additional parts to be inserted. In that case, the printed part will cool down and upon reinsertion into the printer there will be a registration error due to the thermoplastic's expansion and contraction. The registration error includes that the extruded subsequent layers will not be perfectly lined up with the previously deposited layers, resulting in dimensional accuracy errors. Though there is an issue with adding objects such as the magnets or other components, the addition of copper foil to 3D printed parts has issues with manual application, such as accuracy and repeatability. It is of interest because the incorporation of copper foil into 3D printed parts can create products such as heat sinks and antennas. Therefore, through the application of the FA tool, copper foil can be applied to a substrate with an automated tool.

The motivation of the FA tool is to create an automated way to apply copper foil onto a substrate and machine circuits or any other required pattern that may be needed. To reduce the time outside the heated envelope and potential registration errors, the proposed process of the Multi<sup>3D</sup> Manufacturing System will not only eliminate the limitations (i.e., delay and registration errors) but also automate a faster process for 3D printed parts. The end goal is to create a system that will create a product that is 3D printed and contains electrical components, and associated interconnect, within the build upon completion, without manual intervention during the building process.

### **1.3 Thesis Objective**

There are four thesis objectives listed as follows:

1. Design and develop a semi-automated technology that will result in copper foil being embedded within the layers of a 3D printed thermoplastic part.
2. Develop a system that will use copper foil in a process where the end product is a 3D printed part with enhanced capabilities due to conductive material.
3. Discuss the results of the accuracy and capability of the embedded copper foil.
4. Discuss other advantages of the use of copper foil embedded in printed parts.

### **1.4 Thesis Outline**

The following material of this thesis will further discuss the development of the FA tool. The subsequent material is divided into four sections. Chapter two discusses FDM technology as well as a literature review of similar foil applications being developed. In Chapter 3, the design and application of the FA tool is described with justification of the material selections. Chapter 4 provides testing procedures as well as the results on the accuracy and capability of the FA tool. Finally, Chapter five will discuss conclusions of the thesis and present ideas for future work and experimentations to improve the FA tool.



## **CHAPTER 2**

### **LITERATURE REVIEW**

#### **2.1 Introduction**

The conducted research is an overview of the FA tool incorporated into 3D printing applications. Accuracy and capability plays an important part in understanding the effectiveness of this tool. The usefulness of the FA tool is an indication that the tool is a better alternative for foil application compared to previous methods. Furthermore, similar applications and processes will compare and contrast to the methodology of the FA tool. A look at other application processes will validate the prescribed application with the automated implementation of embedded copper foil onto 3D printed substrates.

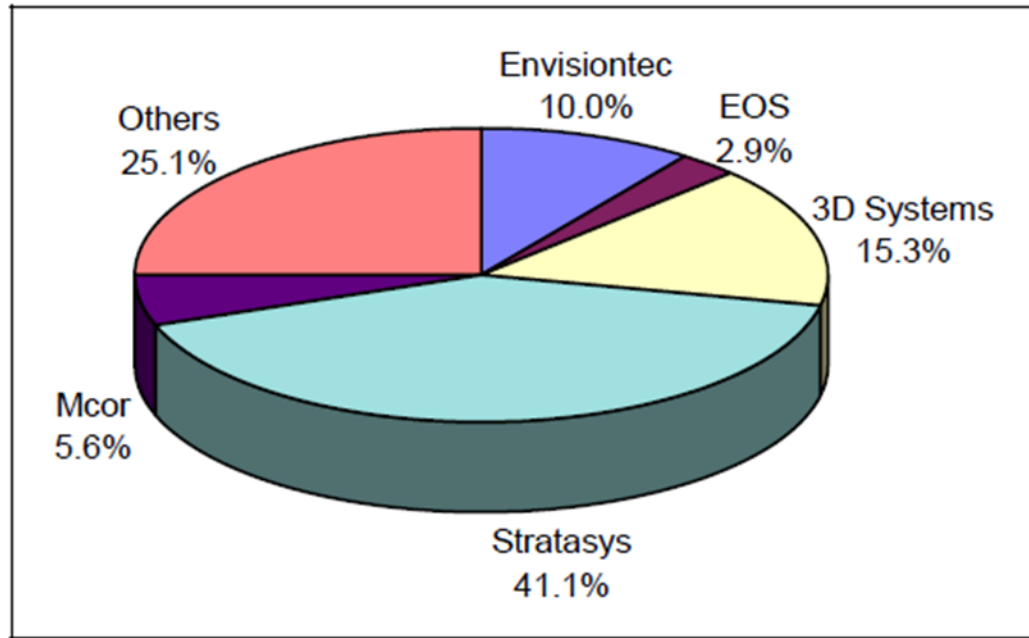
#### **2.2 The Seven Process Categories of Additive Manufacturing**

The American Society for Testing and Materials (ASTM) created seven subcategories for the different AM processes. These seven include vat photo polymerization, binder jetting, powder bed fusion, material jetting, sheet lamination, directed energy deposition and material extrusion. Vat photo polymerization uses a photopolymer resin in a vat and a platform that moves downwards into the pool of resin as a laser positioned above forms the layers. The platform moves down one layers thickness in the vat and another layer is created. Binder jetting is similar in process to the vat photo polymerization in that the platform moves downwards inside the build material. The print head deposits the binding material of the first layer, the platform moves down and a new layer of powder is rolled across the top. The process is repeated until complete. Powder bed fusion and binder jetting share a similar process. The key difference is in using a direct metals laser sintering of electron beam melting to bind the material

instead of a print head to dispense the binding material. This process is used for 3D printing metals.

Material jetting is a type of 3D printer that jets the material onto the build platform. The stream of material will either be in a continuous flow or a more selective drop on demand (DOD) approach. The next type of AM is sheet lamination, used both with plastics and metals; the lamination process binds together stacked sheets of materials through the use of ultrasonic welding or adhesives. As layers of the sheets are added, the required shape is formed by machining or using a laser, leaving behind excess material. Directed energy deposition is a process that both dispenses wire or powder material and is melted simultaneously using a laser, electron beam or arc. This type of printing is for metals.

Lastly, material extrusion, also known as fused deposition modeling (FDM) is the most widely used 3D printing process (Palermo, 2013). This method of printing was used in the following experimentations done for the FA tool. With a heated extrusion tip thermoplastics are selectively dispensed on a layer-by-layer process onto a build platform to create a 3D part. The platform moves downwards as each layer is deposited with either model material, support material or both. The model material is what the finished product is made of. The support material acts as a scaffold to support the object being printed (Palermo, 2013). After the print is complete the finished part is separated from the build platform. Depending on how intricate the design, the support material can be either snapped off by hand or soaked in a solution to remove the soluble support material.



Source: Wohlers Associates, Inc.

**Figure 1.** 2015 unit sales market share estimates among manufacturers of industrial AM systems worldwide (image courtesy of Caffery et al., 2016)

According to Caffery et al. (2016), Stratasys is the industrial leader of sales of AM systems worldwide for the 14<sup>th</sup> consecutive year. In **Figure 1** above, the graph reveals Stratasys as the leading AM manufacture. With a cumulative total of Stratasys industrial systems sold of over 47,000, the company has sold more than double their closest competitor, 3D Systems. Geographically the disbursement of sales around the world has changed since the AM systems first debuted. The United States is the leading country in sales of the total cumulative AM systems sold from 1988 to 2015 with 50.6% of sales in the industry (Caffery et al., 2016). Israel however, sold the most industrial systems in 2015 with 41.1% versus 16.7% in the United States. Since joining the AM community in late 2012, Israel's shares grew along with Europe's and Asia's.

### **2.3 Embedded Electronic Components in 3D Printing**

Rapid manufacturing (RM) is a process that creates end-use products with minimal waste and fast results (Bak, 2004). Since the birth of 3D printing, the design and development of prototypes has changed. The way we create, think, eat and heal will continue to change in the future thanks to the manufacturing processes being developed. This technology is fully capable of generating electronic components that are completely assembled (Kurman et al., 2013). High-performance thermoplastic materials such as PC are used in building 3D models and supports (Priedeman, 2003). With the high performance and nonconductive material PC, this material is well-suited for embedding electrical components such as copper foil due to having more access and background knowledge of the PC material. Copper foil can be used for printed circuits and bonded to a base by using a copper electrolytic bath (Yamanishi et al., 1994). The bath is an electrolyte solution where an electrical charge is sent through the copper to exchange ions (Hochstettler, 1998).

Printed circuits are one way copper foil can be used to enhance a simple non-electric feature. According to Yamanishi et al. (1994) the electrolyzing of a copper foil as a cathode can be done in an acidic copper electrolytic bath. This additional post process changes the copper foil into a material ready for printed circuits. Another way to prepare the copper foil is by etching it. Etching the copper foil removes the top most layer of the coated foil. The removal of the top coat allows for the copper foil to be used with an electrical purpose (i.e. soldering components). The process of etching on the copper foil leaves a laminate staining or discoloration that is a highly undesirable effect (Nelson, 1986). There are other ways the copper foil can be treated without the undesirable discoloration of the material. Multiple copper layer treatments can be done to form a matte surface on the copper foil (Yates et al., 1974). It is

common practice to bond metal foil to a substrate material to form a desired circuit (Yates et al., 1974). According to Ghosh et al. (2009) adhesion is related to the physical effects and the chemical reaction where the coating of the materials and metal meet. Not only is copper foil used for printed circuits but it is also a material used for printed circuit boards (PCB). By passing current from a ground plane on one layer through a hole and onto different features in another layer, all the connected electrical components are in a nonconductive substrate. From this point, resistors, capacitors, diodes, and other components can be soldered onto the copper foil to complete the circuit. The use of a focused laser beam to activate a thermoplastic with copper, nickel and gold is deposited after the print is completed to create a complete circuit track (Huske et al, 2001). The development of the electrical components in the format discussed above were used specifically to create circuit boards.

Testing has been done in the past at the Keck Center with the inclusion of electrical components. Aguilera et al. (2013), inserted electronics into partially fabricated structures. The fabrications required pauses to allow for the embedding of multiple different components to create a motor. The end result of the inserted electronics into the 3D printed parts was a single structure built with multiple components sealed inside. The Keck Center has conducted experiments on similar grounds in the past with various copper materials. Sensors were made using PC, single copper wire and fine-pitch copper mesh (Shemelya et al., 2015). Very close to the materials used with the FA tool, testing the PC and various copper materials show capabilities in creating electrical components. Shemelya et al. (2015) created specimens where microcontrollers, capacitors, resistors diodes and LEDs were fully embedded into the substrate to create a capacitive sensor. The Keck Center has also created spiral antennas with the use of the PC material (Shemelya et al., 2016). The antennas required the embedding of copper for a

ground plane. The use of copper wires thermally embedded into 3D printed thermoplastic materials were also tested (Marquez, 2016). According to Marquez (2016), the copper wires were used as conductive traces for electronic applications. Other hybrid manufacturing (HM) systems have also been developed to create 3D printed parts with embedded electrical components. A process was created to fabricate 2D and 3D monolithic structures with embedded electronics and circuitry (Lopes et al., 2012). With LEDs and other various electronic components embedded to respond to changes in temperature (Lopes et al., 2012).

HM systems are an inclusion of various processes to combine different manufacturing processes with similar objectives of improving surface integrity, increasing material removal rate, reducing tool wear, reducing production time and extending application areas (Zhu et al., 2013). The HM process is not restricted to one type of system; there are multiple types of HM systems for various applications. A laser aided manufacturing process (LAMP) was created with a five axis HM process, complete with in house CAD software (Nagel et al., 2012). Another example of an HM process was a repurposed six axis robotic arm that was used to incorporate a seamless integration of additive and subtractive manufacturing by mounting the platform of a build to the robot and transitioning the build between the two manufacturing systems (Keating et al., 2013). There are many different ways an HM process can be created. With multiple manufacturing processes and an improvement to an existing system, many systems can fall under the HM process.

The layer by layer extrusion of the PC in the 3D printing process gave way for all of the above mentioned embedding applications. Pausing the print at one or multiple layers allowed for multilayer embedding. The use of copper foil in an AM process has been discussed as a way to improve the manufacturability of a printed part with added electrical capabilities. The HM system has also been discussed as a way to combine different

manufacturing processes to create one system that integrates multiple processes to improve manufacturing. The inclusion of this tool into the Multi<sup>3D</sup> Manufacturing System can create a faster end-use part with electronic components.

## **CHAPTER 3**

### **FOIL APPLICATION TOOL**

#### **3.1 Concept**

The concept of the foil application (FA) tool was to create a technology capable of embedding copper foil while simultaneously limiting human interaction in the process. The FA tool allows for a process of applying copper foil on one or more of the interlayers of a 3D printed specimen. Copper foil possesses multiple electronic uses which include, but are not limited to: circuits with a minimal thickness, pathways for thermal transfer, radiating elements and ground planes for antenna applications. The foil can be applied and then machined into any design deemed necessary. The sections within this chapter will further discuss the development of the FA tool.

#### **3.2 Design Objectives**

Design objectives were recognized and prioritized and are shown as follows;

1. Design and develop a tool that can apply copper foil in an adjustable automated system that can produce a repeatable specimen.
2. Automate all components of the tool
3. Allow for customized patterns to be cut out of the copper foil for multipurpose use
4. Design all of the components in an iterative fashion so that components can be interchanged quickly if necessary for design or maintenance purposes
5. Design the tool to be mounted on the tool changer to accommodate the housing space for the tool when idling



### **3.3 Design Constraints**

The design of the FA tool had to accommodate many constraints for the tool to be successful. The constraints for the FA tool were size and temperature. When designing the tool size, constraints were given to not exceed 127 mm wide and deep, the “z” height could however have a variable size. These size constraints were given specifically for the tool stand dimensions. The Multi<sup>3D</sup> Manufacturing System had the capability to accommodate various tool heads incorporated into the machine. The space allotted for storage of the different tool heads when idling was also integrated into the design. The next constraint was temperature. The heated envelope of the machine could reach up to 200°C. The exposed components of the tool needed to withstand the temperature without being compromised. The tool was fabricated with the intent to minimize weight.

### 3.4 Iteration of Design

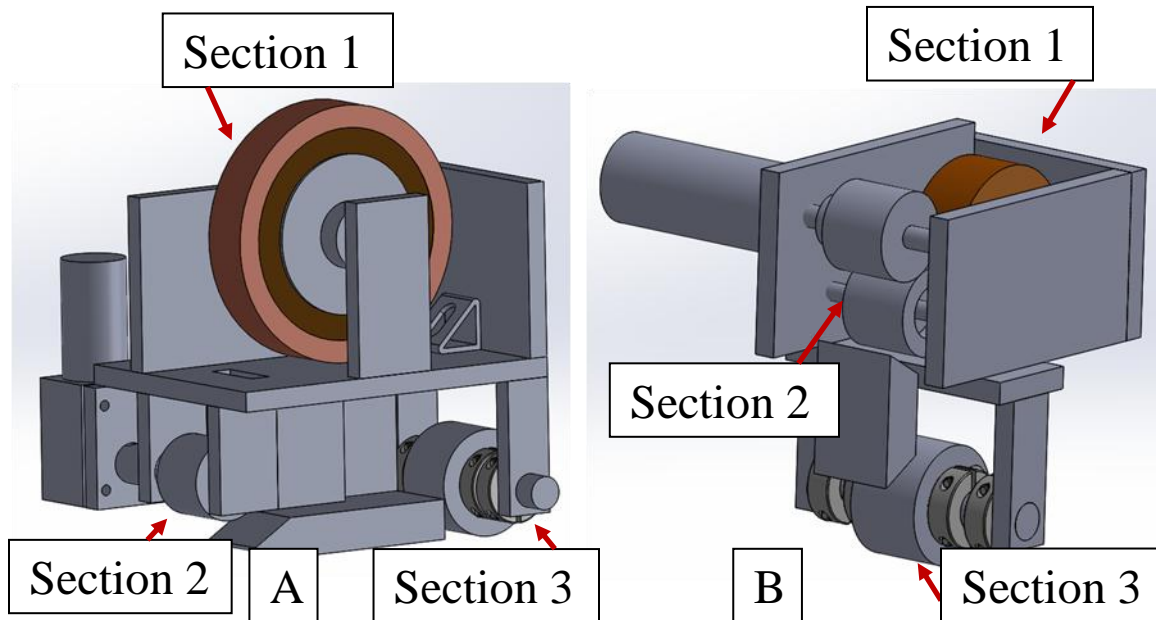


**Figure 2.** A) First manufactured design of the FA Tool, B) iterated design of the FA Tool

The initial design of the FA tool had three sections in which the foil makes it from the spool onto the substrate. The initial section was the copper foil mounted onto the upper part of the FA tool. It was attached to a roller mounted on a shaft. The shaft was attached at either end with one way locking bearings. This allowed for the foil to only be unraveled in one direction, towards the pinch rollers. On its way to section two, the foil was put through the slot in the horizontal base plate. The slot was strategically placed and sized to allow for the foil from the spool above to be fed into the pinch rollers below consistently. Section two of the foil application was the pinch rollers. These rollers provided the power and tension needed to pull on the foil from the spool and feed it to the roller that would apply it to the substrate. The pinch roller consisted of two rollers, a driver, and an idler. The driver, as shown in **Figure 2** was attached to a motor that would rotate the drive roller. The idler roller made contact with the drive roller and rotated as the drive roller moved. These two rollers pulled the foil downwards

into a channel that guided the foil to the roller. This guide was there to maintain the level at which the foil met the roller as well as to keep a consistency in the placement of the foil in reference to the roller. The third and final section took the foil from the guide to the roller that applied it to the substrate below. High temperature adhesive was added to the substrate before applying the foil. Excess foil that was not needed was machined off later.

The FA tool was designed in such a way that fulfilled all of the component functionalities: to apply the copper foil. However, the FA tool did not meet the size criteria initially prescribed. The initial size of the tool was 193.55 mm x 172.21 mm x 210.06 mm, much larger than the 127 mm requirement. The reason for the size increase was to accommodate the copper foil spool which had an outer diameter of 127 mm. The spool dimension was already the maximum size for the tool criteria. The copper foil still needed to be fed through the pinch rollers driven by the motor. These components added to the height and length of the 127 mm spool. The copper foil spool could not be located too closely to the mounting plate, an Allen Wrench needed access to a bolt behind the spool.

To remedy these size restraints the new design featured collar clamps as shown in **Figure 3** below. The original design required press fit shafts and custom welds that would render the whole assembly unusable if a part needed to be replaced. This new design allowed for either the collar clamps or the set screws holding the vertical supporting beams to be removed. All of the individual parts could be accessed and changed with little down time and replaceable parts in an easily accessible location.

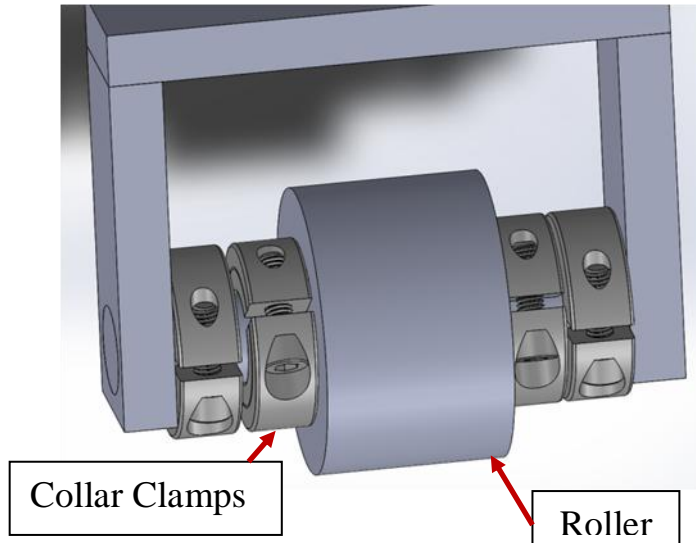


**Figure 3.** Roller sub assembly

The first possible need for improvement was noticed when working with the initial design of the tool. Replacing components was a difficult task. There was a layered format on how to change out a part on the FA tool, such as the removal of the roller. This was a procedure that needed to be done for cleaning purposes as a result of excess adhesive adhering to the roller while undergoing the application of the foil. The task to remove bolts and numerous plates was deemed unnecessary. This was due to the fact that there were too many components.



**Figure 4.** Roller with excess adhesive after application

In the initial design stage of the tool, the amount of plates and bolts, as well as their functionality and ease of interchangeability was neglected. The subsequent design of the FA tool took this into consideration by changing the associability of the components. The result was minimal amounts of plates, where almost all of the bolts could be accessed without dismantling other components. The change minimized the amount of plates from 12 to 7. It also eliminated excessive amounts of bolts lightening the weight of the tool and shortening the time it took to replace parts or conduct maintenance.

The pinch roller system was created to drive the foil from the spool into the guide and to the roller. In the first design the pinch rollers were below the copper foil spool and in line with the roller, the guide in between them. However, the rollers were made of Urethane and only had a temperature tolerance of approximately 93°C, less than half of what the temperature could reach in the envelope (200°C). The Urethane rollers were suggested to be used at 93°C by the manufacturer as the maximum operating temperature. To accommodate the temperature

increase, the design was modified so that the pinch rollers were moved to the top half of the tool with the copper foil spool and the motor; instead of using high temperature and more expensive custom rollers. Components that could withstand high temperatures were placed below, exposed to the heated envelope.

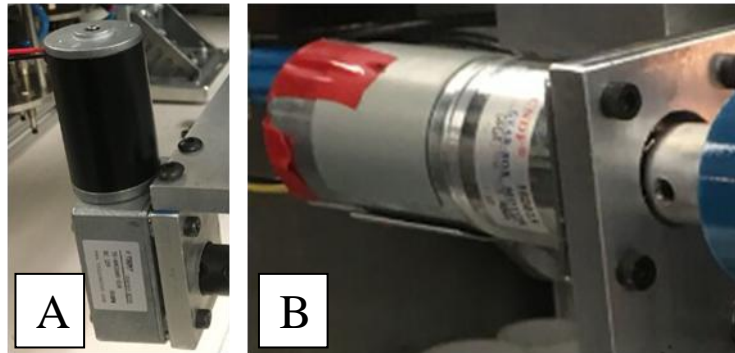


**Figure 5.** A) TSINY Gear Box Motor with a lower torque, B) final motor with a higher torque

The first motor was chosen due to its gear box, a more compact version that would decrease the width of the tool. To overcome the friction of pulling the foil from the spool at a slow rate of 254 mm per minute or 4RPM, a higher torque than that of the gear box motor (14.7 Kg-cm) was needed. A new motor was added to the subsequent design shown above in **Figure 5 B** that was stronger (20.9 Kg-cm) and could overcome the resistance. The new motor was longer than the other motor and would increase the width of the tool above the heated envelope. The increase in dimension of the tool was a necessary compromise.

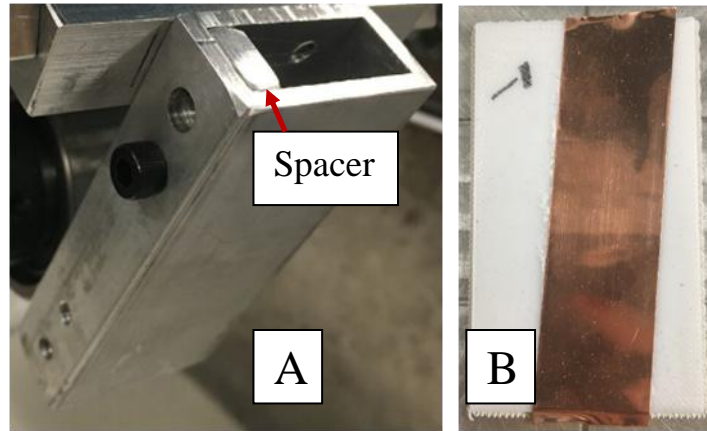


**Figure 6.** A) Guide with spacer, B) crooked applied foil

It was made clear right away through preliminary testing of the FA tool that a guide was necessary. Initially the guide was placed to keep the foil from falling or sagging before reaching the roller. However, the tests revealed crooked application samples. The guide therefore needed iteration with an interchangeable size adjustment. A small bar was inserted into the foil guide leaving a 26 mm width in the guide, just enough for the cooper foil to pass through without misaligning. The thickness of this spacer could be interchanged with other spacers to keep various sized cooper foil aligned with a width of 25.4 mm or less. The roller could only accommodate up to a 25.4 mm width. Anything larger than that would require a larger roller and a wider guide, both of which would have changed many aspects of how the tool was constructed.



**Figure 7.** Side view of the spring loaded roller

Another feature that was added to the FA tool was the spring loaded roller. This was added due to a realization that the roller was not always aligned with the substrate, resulting in only part of the copper foil being applied onto the substrate; the other part never touched the PC. To remedy this slightly crooked apparatus, a spring loaded feature was added. The spring connects the horizontal base plate to the vertical plate that secures the roller's location through a bolt. When the roller was placed onto the substrate with some pressure the springs on both sides would compress to ensure that all of the copper foil would touch the substrate.

The large copper spool was changed in the iterated design due to its large scale and inability to minimize the size and location of all the other components. The original dimensions of the spool were: outer diameter (OD): 127 mm and an inner diameter (ID): 76.2 mm. The spool was re-spun onto the 19.05 mm metal shaft that held the original copper foil spool with the one way locking bearings. The new dimensions of the Copper foil were OD: 69.85 mm and an ID: 19.05 mm, thus making the outer diameter of the re-spun spool smaller than the inner diameter of the original spool. Not only did this change the weight of the tool by eliminating the



hub connecting the copper foil to the shaft but it also reduced the size greatly, allowing for a smaller iterated tool.

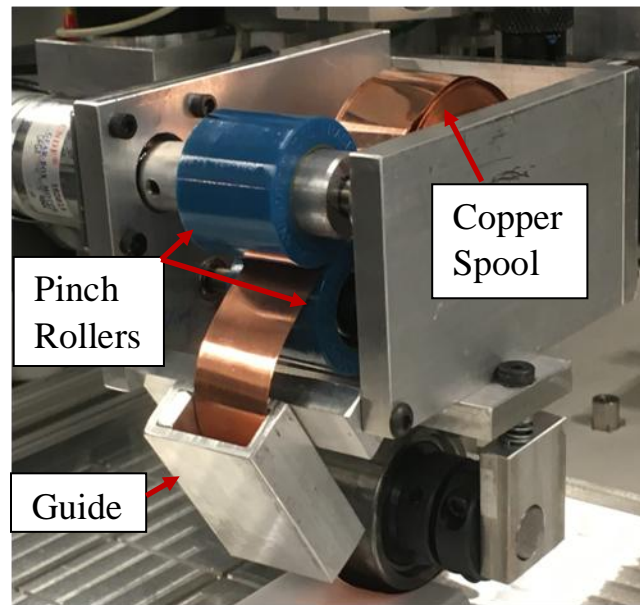


**Figure 8.** Design two of the FA Tool applying copper foil onto a substrate

The image shows the new model of the FA tool as it was applying the copper foil for the first time. The copper foil spool was condensed by rolling the inner diameter of the spool onto a smaller shaft. Taking advantage of the size reduction, the pinch rollers were oriented in a diagonal fashion to better feed the foil into the guide as well as lower the overall height of the tool. The lower half of the FA tool contained only the necessary components to apply the foil including the roller and the guide. All other components were on the top half of the tool. This design change created a separation of the upper and lower half based on temperature limitations. The bottom half was exposed to the heated envelope. The upper half, to include the motor, was thermally insulated.

### **3.5 Material and Component Selection**

All structural components of the FA tool from the base and mounting plates to the shafts supporting the rollers and copper spool were Aluminum 6061. Besides the ease of accessibility of Aluminum 6061, it is easy to machine relative to other materials such as steel. This material was beneficial during the design process because changed components could be machined quickly and easily.

The copper foil chosen was a 25.4 mm wide by 30.48 meter long roll with a thickness of 0.127 mm. This foil was chosen due to its availability through different suppliers. Refills could be purchased in the future of the same type of copper foil to keep a consistency between testing results without varying the type of material. The bearings controlling the movement of the copper foil spool were one way locking bearings. Press fit into the aluminum side plates, these bearings only rotated in one direction that fed the foil from the spool and to the pinch rollers.

The pinch rollers were made of Urethane and Aluminum with a diameter of 38.1 mm and a width of 31.75 mm. These rollers did not meet the temperature requirements; they were only able to reach up to about 93°C. The rollers were still chosen with the expectation that the design had to incorporate the pinch rollers in the enclosed upper part of the tool instead of the exposed area below, a constraint that guided the changes in the design iteration. The alternative would have been two custom made pinch rollers that could withstand the temperature requirements but were also more than twice as expensive and had a lead time of over a month. Choosing the latter option would have made it more difficult in the future to maintain or exchange the roller. The urethane rollers were readily available and the design changed to accommodate the rollers in the upper cooler compartment.

Throughout the development of the FA tool two different motors were used. The first was the TSINY Gear-Box Motor, a twelve volt DC motor capable of up to 35RPM. This motor was chosen due to its qualities of being oriented perpendicular with a gear box. Ideal to the design of the FA tool to minimize the width of the tool, with a torque of 14.7 Kg cm however, the TSINY motor was not able to overcome the resistance of the weight of the copper foil spool at a slow speed of 4RPM. The new motor chosen, although not a gearbox motor, was able to overcome the friction of the spools weight with a torque of 20.9 Kg cm. This motor was also a twelve volt DC motor with the capability of 10RPM. Despite its substantial addition to the width of the tool, the application of the motor was needed to run the FA tool.

The guide was a 38.1 mm by 19.05 mm aluminum rectangular tubing. The thickness of the tubing was 3.18 mm. At 57.15 mm long, the guide fed the copper foil from the pinch rollers to the exposed roller below. An adjustable aluminum spacing bar was inserted along the length of the inside of the guide to maintain a 25.4 mm wide gap throughout the guide. This rectangular tubing was chosen due to its capability of maintaining the integrity of the copper foil and directing the foil towards the roller without a chance of the foil escaping the guide.

The roller chosen for the FA tool was a Yoke Type Track Roller. Being that this roller would be exposed to the heated printing envelope, the ability to withstand the high temperatures lead the search for this roller. With a diameter of 50.8 mm and a width of 31.75 mm the roller had a temperature capability of 177°C. Another component chosen for the FA tool was the shaft collars. These two piece black oxide 1215 Carbon Steel collars were placed two on each side of the roller, one on the shaft and against vertical mounting plate and the other against the roller. The collars were strategically placed to maintain the rollers and shaft's position in reference to the mounting plates.

Other components chosen for the FA tool were the chemicals for adhesion and post processing of the applied foil. The selection of the adhesive began with a series of tests to determine the best adhesive for the foil application tool process. The first criteria that needed to be fulfilled was a high temperature adhesive that could withstand the 200°C temperatures. At this point two different types of adhesives posed as the most compatible, an epoxy and a liquid form similar to super glue. The epoxy was ruled out because the combined height of the copper foil and the epoxy would create an obstruction for subsequently printed layers. Therefore, the liquid glue was chosen. Two different high temperature adhesives were tested with different application processes. Small sample pieces of copper foil were glued to PC parts with different temperature applications. One test applied the adhesive to a room temperature part and then was placed in a furnace to simulate the printing process. In another test the adhesive was applied to a PC part at room temperature and then left at room temperature. In the last test the PC part was placed in the furnace before and after the adhesive application. The adhesive's best form of application was the last test where the part was heated before and after the application. Therefore, through the short testing process the adhesive for the application was chosen. Both adhesives showed effective adhesion when applied after waiting for the substrate to cool for ten minutes. Although the other tests that did not adhere as well with either adhesive revealed that one was stronger than the other in the bonding qualities; resulting in the selection of an adhesive that fit many of the qualities needed. The adhesive chosen was the Permabond Engineering Adhesive Instant Adhesive 820 High Temperature Peak +200°C.

The etchant used to etch the copper foil was the PCB Etchant Solution Full Strength Contains Ferric Chloride. This was a common etchant used for PCB made with Ferric Chloride, a material used for etching copper and was chosen over in house made etchant for convenience.

Isopropyl alcohol was used to clean the copper after applying the etchant and before applying the ABS solution. ABS solution was made with small particles of ABS mixed with acetone to create a thick liquid substance. The solution was applied to the surface of the Copper before subsequent printing occurred to create a sticky layer above the slick copper foil so the PC printed and the copper layers meshed together.

The accelerant was the last component to be selected. The need for accelerant was discovered after multiple applied foil strips were not adhered when the roller applied the foil onto the substrate. The FA tool could apply copper foil along the length of a 76.2 mm substrate in under ten seconds. The adhesive however took over 30 seconds to dry after application, 20 seconds after the copper foil was already applied. The excess material at the top of the PC part was held onto as the foil was being applied to keep the foil from sliding down. To remedy this slippage, accelerant was used. Multiple types of accelerants were tested with different spray tips. The accelerant chosen was the Loctite SF 713 Accelerator. With a spray nozzle, this accelerant displayed full coverage, the adhesion time changed from approximately thirty seconds to under ten. The accelerant allowed for the foil to be applied without the need for the top of the foil to be held because there was no slippage of the foil. Once applied, the foil stayed in place regardless of the small resistance exerted from the FA tool.

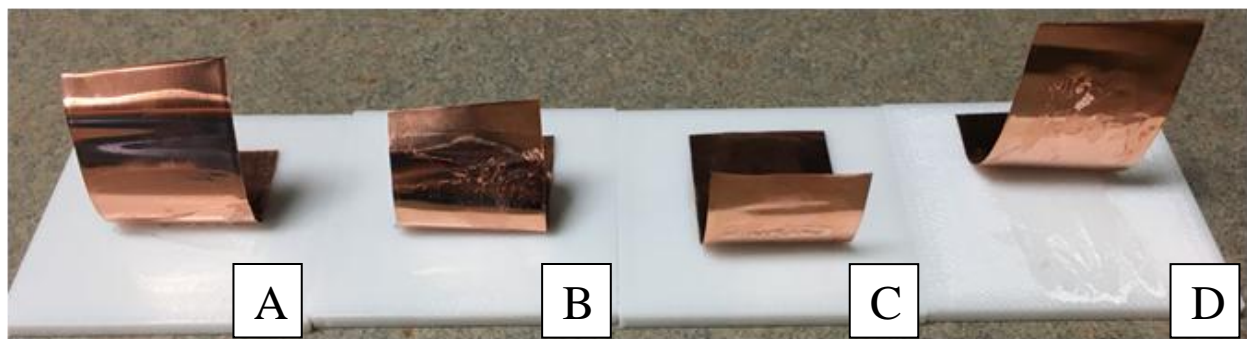


**Figure 9.** Initial testing of adhesive with accelerant

The results of the experiments in **Figure 9** displayed the four different test specimens used to clarify which sequence of application would best adhere the two materials (adhesive and accelerant). Starting from the left, the first test of the PC sample had the accelerant and the adhesive applied one after the other immediately after being removed from the printer. Taking cues from previous testing the second test was done by adding the accelerant immediately after removing from the heated envelope and then waiting ten minutes before adding the adhesive and the foil. The second test adhered more effectively than the first. The third test resulted in the strongest adhesion of the four tests, where the substrate was left alone for ten minutes to cool down before adding the accelerant, adhesive and foil. The fourth test as seen in **Figure 9 D** was the application of the two chemicals after the PC was cooled to room temperature. This resulted in the least adhesion of the four with little resistance when peeled off. After the initial tests, the third application method was used with the foil application tool.

### **3.6 Application and Embedding Process**

The FA tool was a system that applied copper foil along the X-axis. Although the tool could move in all three (x, y, and z) directions, it was set up so that the copper foil was dispensed exclusively using only two directions, vertically and along the length of the substrate. To align the tool on the substrate the following steps needed to be taken:

- Align the tool to the appropriate location in the x and y-axis
- Zero the tool at the starting location
- Determine the “Z” height by pressing the roller down on the substrate with the copper foil in between

- If the springs on either side compressed slightly then the foil was touching at all points along the length of the roller.

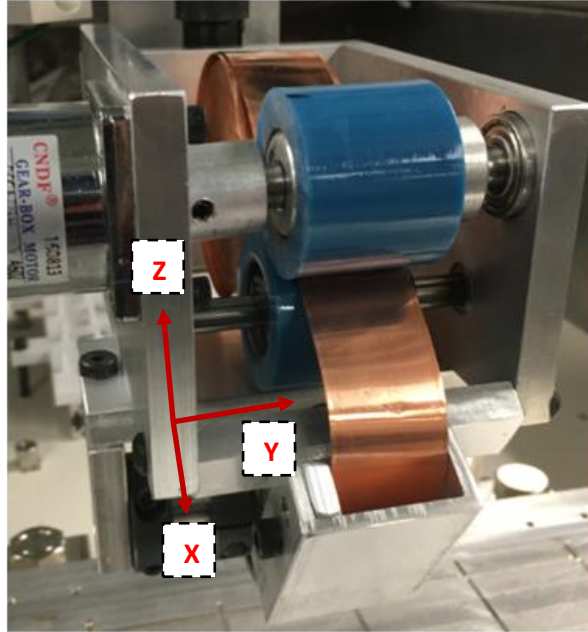


**Figure 10.** FA Tool with labeled axes

Before beginning any of the steps to create a part for which copper foil would be embedded, first the desired copper foil design and dimensions were established. After creating the CAD file, the part was sent to the printer with the pause needed to apply the foil. When the substrate was printed the six-axis robot removed the platform from the FDM2 printer and placed it in the CNC router for further tooling where the FA tool was installed onto the gantry and ready for use.

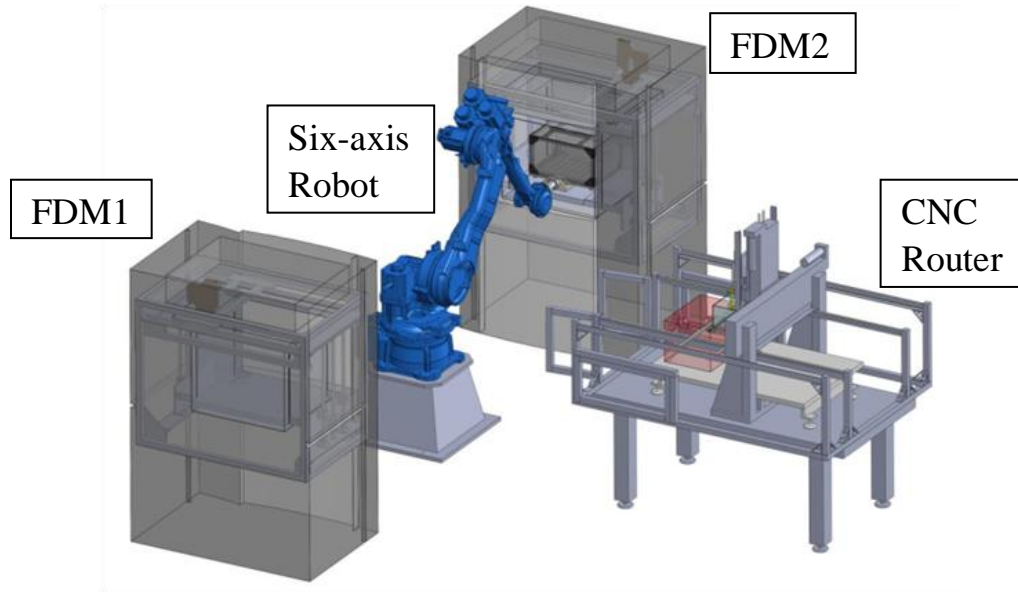


**Figure 11.** Multi<sup>3D</sup> Manufacturing System (Ambriz, 2015)

The PC part needed to cool for ten minutes before beginning the application process. After the allotted time the accelerant was applied to the substrate followed, by the adhesive. As the adhesive was being applied so was the foil. If the foil was applied after all the adhesive was dispensed, the adhesive hardened and caused the copper foil to have a rough, surface finish. The results of a sample PC part after applying the copper foil was shown in the image below. In this test all of the adhesive was applied before the FA tool began to apply the copper foil, resulting in the adhesive drying before the foil could cross the entire sample. The rough texture and lack of adhesion on both sample pieces was due to the adhesive drying too quickly.



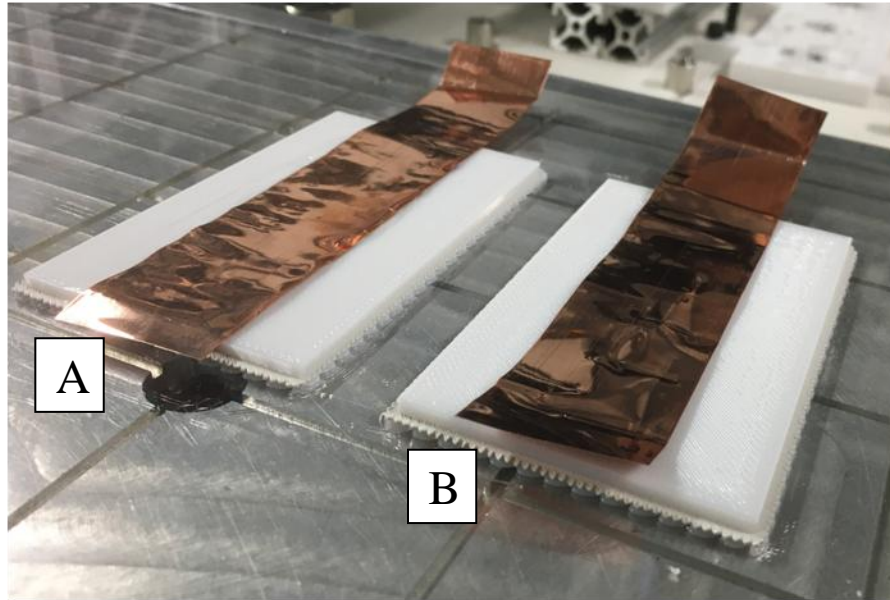


**Figure 12.** A) Left sample of foil after being applied with accelerant, B) right sample of foil after being applied with accelerant

Post processing took place after the foil had been applied and the foil was cut to separate the applied foil from the foil in the FA tool, this process added a few additional steps to the sequence. The excess foil at both ends was removed, leaving behind only the foil on the PC. For instances when the applied copper foil needed to be exposed without subsequent layers to print over it, the process stopped there. If subsequent layers of PC were to be printed above the applied copper foil as in most cases, further steps needed to be taken. For the three following chemicals, etchant, isopropanol, and ABS solution cotton swabs were used to dispense the liquids onto the applied copper foil. The etchant was applied followed by the Isopropanol.

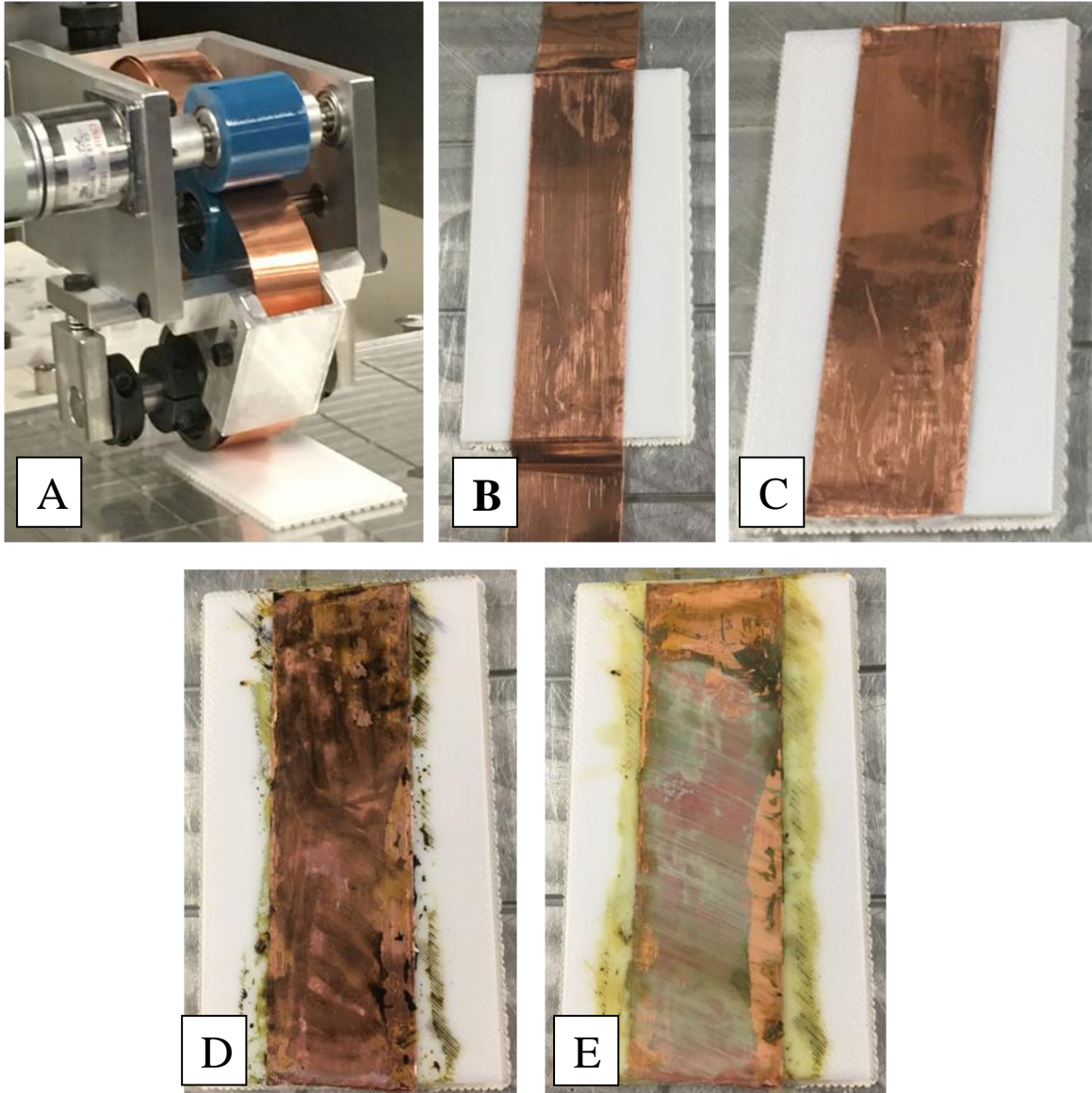


**Figure 13.** A) FA Tool applying copper foil, B) applied foil after FA Tool was removed, C) excess material was removed, D) etchant was applied to copper foil, E) isopropanol added after etchant

The six-axis robot then lifted the platform and returned the part to the FDM2 printing envelope. The sample was left to heat up in the envelope for ten minutes, ABS solution was applied to the surface of the copper foil. ABS solution varied between two different colors throughout testing, one was black and the other white. The images below show the difference in

using both colors. The white solution gave the best results aesthetically, the copper foil was slightly visible through the subsequent layers of PC instead of the black solution that completely covered the copper foil and left a messy residual texture. It was recommended that similar colors be used for the printed material and the ABS solution. The print was then resumed and additional layers of PC were printed on top of the applied copper foil. The finished product was a PC part with copper foil embedded within the layers.

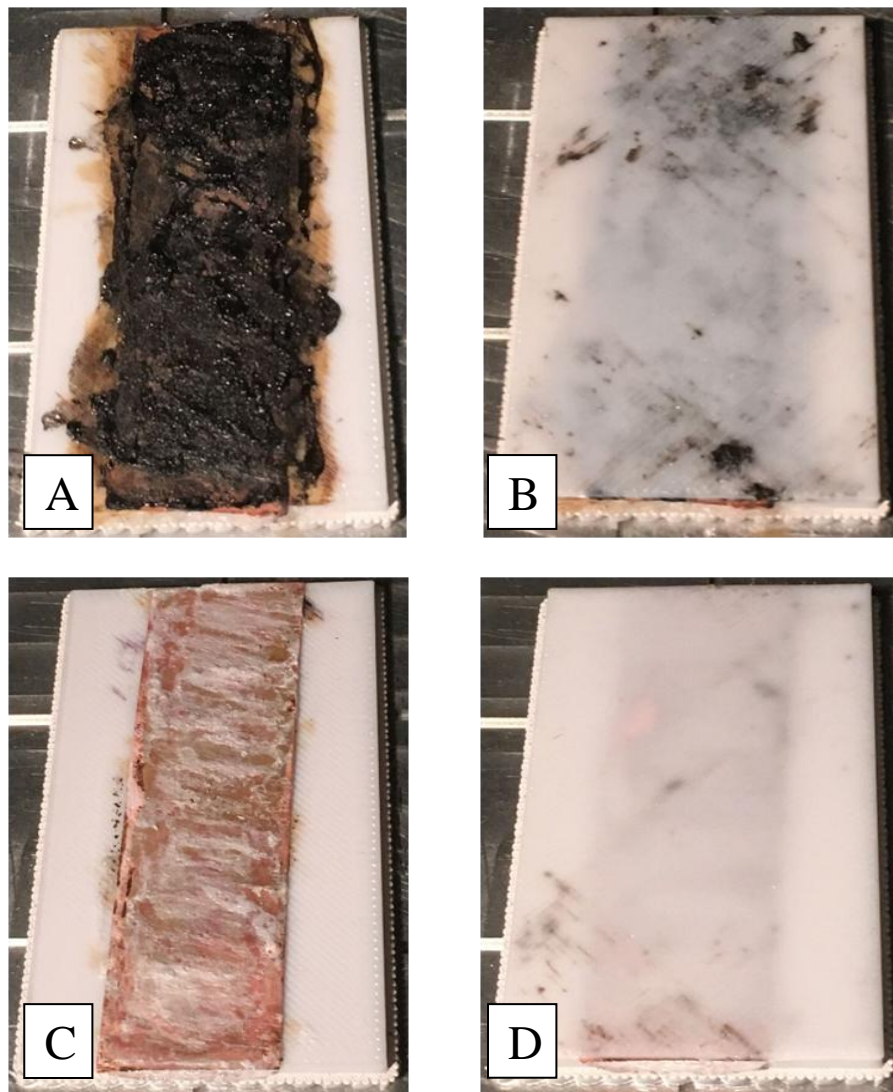


**Figure 14.** A) Black ABS Solution, B) resulting part, C) white ABS Solution, D) resulting part

## CHAPTER 4

### DESIGN EVALUATION/EXPERIMENTATION

#### 4.1 Demonstration: CNC End Mill Cut Out of Patterns

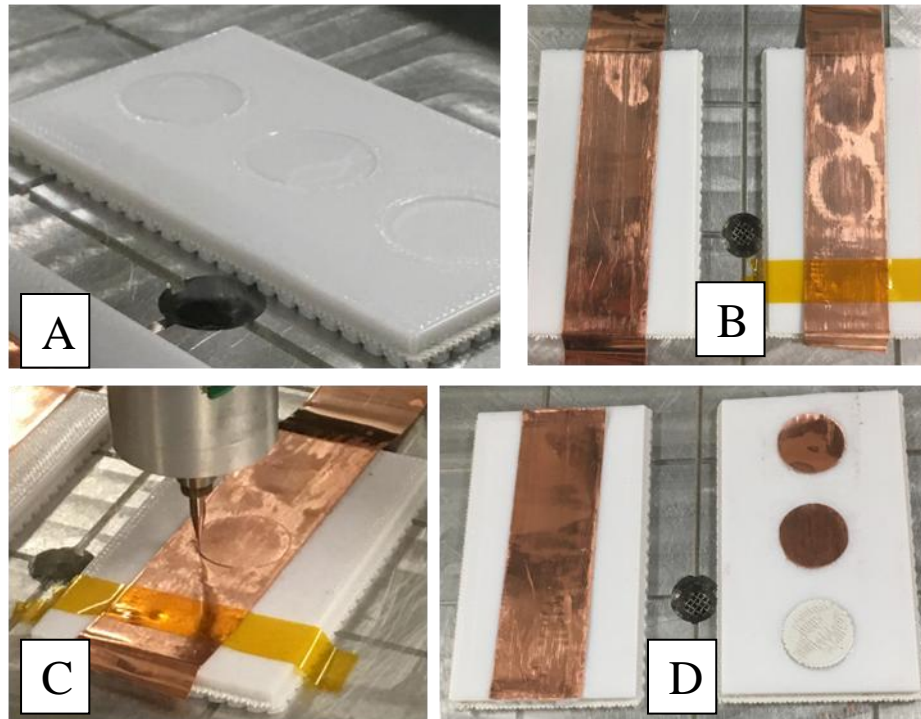


**Figure 15.** A) Printed substrate with indentions, B) post application, C) CNC Router cutting out preprogrammed shapes, D) resulting applied copper foil

The process of cutting the foil into different patterns was shown in the image above. The possible designs to be created with the cooper foil were only limited by the capabilities of the end mill. After the end mill had cut through the cooper foil, the excess was pulled away to reveal only the desired material. As seen in the image above the substrate already contained the pattern of the copper foil design. This was not necessary, the end mill was preprogrammed to cut the design with or without the indentation. Tests revealed better adhesion results when the substrate had a smooth even surface without the indentations.



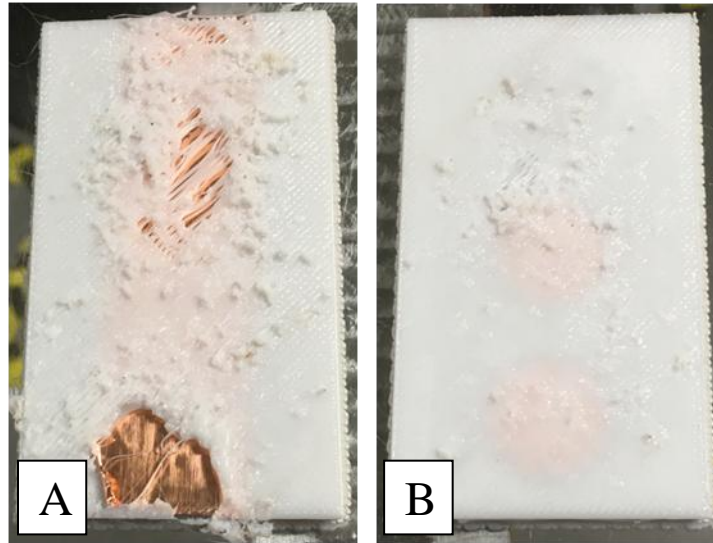


**Figure 16.** A) Full width copper foil strip applied and printed over without post process chemicals, B) cut out of circular patterns and printed over without post process chemicals

The first test conducted with the FA tool was shown in **Figure 16**. The application of the foil was successful as well as the cut out of two circular patterns. A post process of adding the etchant, Isopropanol and ABS solution were not applied to these specimens. The result was a rough finished texture of PC and in many places, exposed copper foil. The test was done again later with the same settings and application method as in this previous test, however the post processes chemicals were applied. Results were much better and can be seen in all other test specimens.

## 4.2 Testing

The test specimens were designed to best display the testing application. There were multiple different types of tests and equally as many different substrates. The first specimens were to test the capability of the FA tool. These specimens were simple user specified dimensions 50.8 mm by 76.2 mm samples of PC where 25.4 mm wide copper foil could be

applied with a 12.7 mm leeway on each side and a 76.2 mm span. This was made to test that the FA tool could apply the copper foil. This specimen was used for initial application validity test and the following test.

The first test used similar substrates with a three point bend flexural test. The Instron material testing machine was used for the tests. All of the test specimens were measured and marked before testing and were placed in the same location on the Instron. Three PC test specimens were printed with the inclusion of the pause where the foil would have been applied, although it did not have any embedded foil. After the completion of the print and cooling to room temperature, the specimens were placed in the Instron for the three point flexural bend test. The Instron used a displacement rate of 5 mm per minute on the test specimens. The second set of specimens were embedded with 12.7 mm wide copper foil, half the width of the foil size. The embedding of the foil was done on layer eleven of the fifteen layer test specimen. The side of the test specimen with the copper foil closest to the surface was turned downwards in the flexural three point bend test. Doing so created a test where the side with the copper foil had more surface area contact during the test. The last set of test specimens for this test were embedded with the full width of the copper foil of 25.4 mm. Similar to the 12.7 mm foil, the samples were tested with the copper side facing downwards.

For the next testing apparatus the specimen was very similar to the previous with the same dimensions of 50.8 mm by 76.2 mm, however the subsequent layers of PC were eliminated. The “Straightness Test” featured five specimens where copper foil was applied onto the PC substrate. For the purpose of measuring the distance from the copper foil edge to the edge of the substrate on either side, subsequent layers were not printed thus removing the need to dispense the post process chemicals.

Another experiment was done with a substrate that was created with a similar concept to the previous test with a different pattern. This specimen was a 76.2 mm by 76.2 mm by 12.7 mm tall. At every 2.54 mm (ten layers) a pause was inserted for a total of four pauses. The purpose of this test was to find out how closely the foil could be applied to the same two spots repeatedly at different layers. After the part was embedded and printed it was sliced into five equally sized parts to gain five slices for measurements along the length of the test specimen.

The last test was the “Heat Transfer Test.” The “Heat Transfer Test” was created with a purpose of determining how well the copper foil could transfer applied heat from one side of the PC part to the other. Below in **Figure 17** the copper foil was being applied to the heat transfer part. Although only being applied to side 2, excess foil was left attached on both sides to cover side 1 and 3. Before securing the copper foil on side 1 and 3 with adhesive the thermocouples needed to be attached. As seen on side 1 in **Figure 17** there are three slots for the thermocouples each one corresponding to a strip of foil, the left middle and right side. Side 1 and 3 each have slots for three thermocouples, one for each strip. Side 2 has nine, three for each strip, creating five thermocouples for each strip, totaling 15 thermocouples.

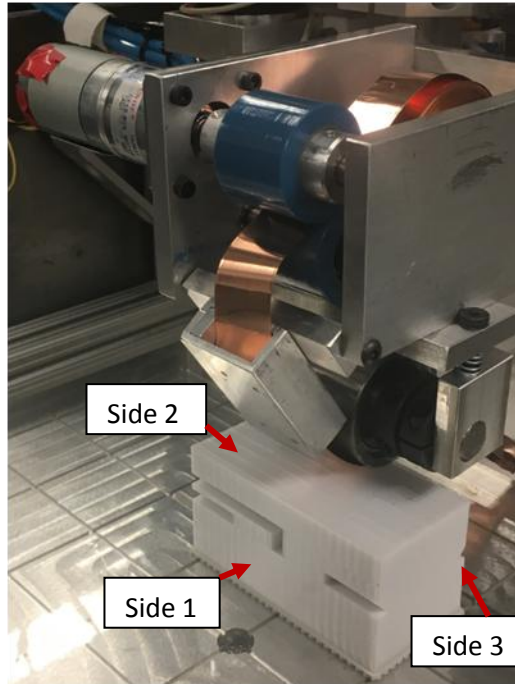


**Figure 17.** Applying copper foil to heat transfer part

After applying the copper foil the post processing chemicals were added to ensure the subsequent layers would adhere properly. One more layer was added to show the layout of where the thermocouples would be applied onto the part. A cotton swab with Isopropanol was used to remove the ABS solution covering the copper foil to help the thermocouples maintain direct contact with the copper foil. The nine thermocouples applied on side two of the heat transfer part were adhered to the PC part with the same high temperature adhesive used on the copper foil. The adhesive was necessary to keep the thermocouples in place because subsequent layers would be printed, resulting in embedded thermocouples.



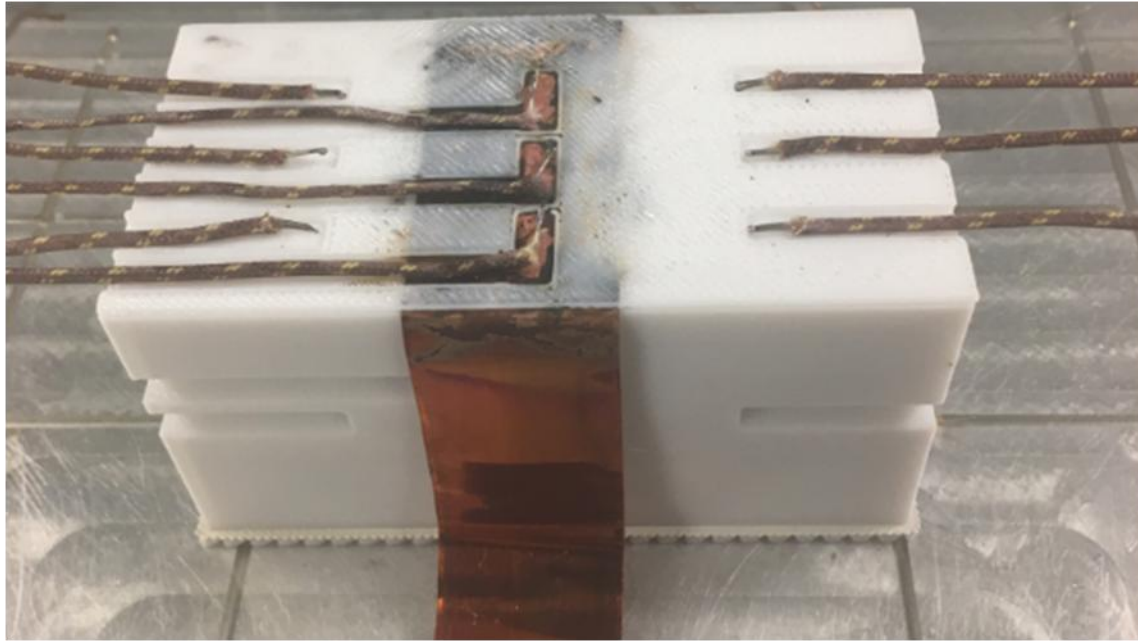


**Figure 18.** Thermocouples attached to heat transfer part

**Figure 19** shows the testing apparatus for the heat transfer test. **Figure 19 A** and **C** shows the DAQ system that was connected to the heat transfer part via all 15 thermocouples. The DAQ system was also connected to a computer where all of the data was collected and exported into an excel file. **Figure 19 D** shows the heating plate. **Figure 19 B** shows the thermal paste used on the face of the heat transfer part that was placed on the heating plate. The plate was used to reach the glass transition temperature of PC, 147°C.

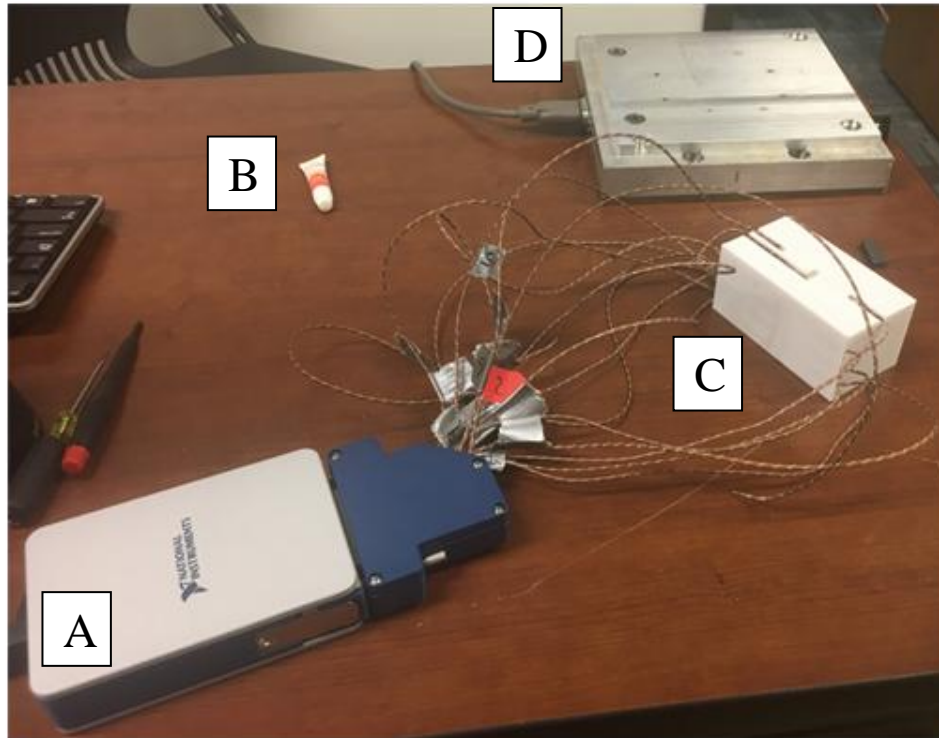


**Figure 19.** Testing apparatus, A) DAQ system, B) thermal paste, C) heat transfer part, D) heating plate

The experiment was conducted with side 1 applied with the thermal paste and placed directly onto the heating plate, subsequently side 3 was furthest away from the heat source. Before testing began, the heating plate had to be at room temperature to ensure repeatability for the other test specimens. The DAQ system then started to take measurements immediately after the heating plate was turned on. Measurements were taken every second for an hour, 3600 measurements for 15 thermocouples. After the hour was completed the DAQ system was stopped and the heating plate turned off to begin cooling in preparation for the next test.

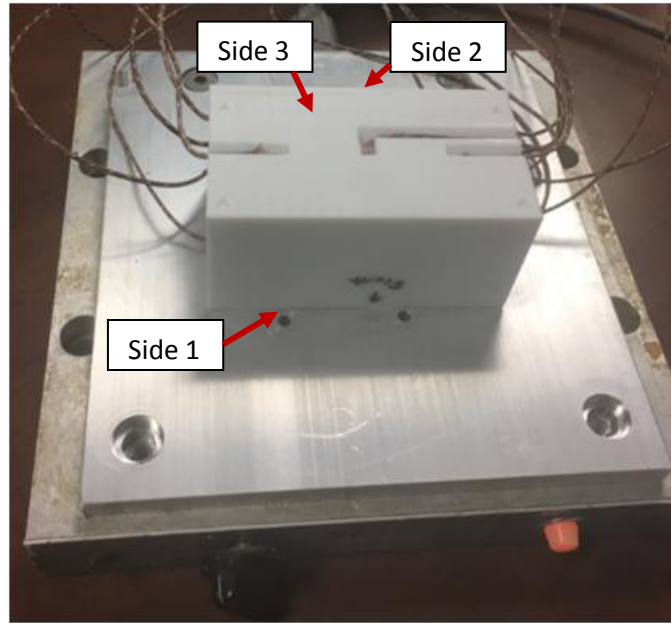


**Figure 20.** Heat transfer part placed onto heating plate

To keep the foil strips centered on the four different test specimens the copper foil was applied as follows: For one foil, the strip was placed in the center; for two foils, copper foil was placed on the left and right strip leaving the center strip without foil. Lastly, the three foils covered each of the strips, leaving none of the thermocouples exposed. The data in the graphs were collected using the thermocouple data from the center strips for the no foil, one foil and three foil specimens. The two foil specimen did not have a center strip of copper foil, therefore the data collected for the two foil specimen was from the left side strip.

### **4.3 Results**

The following results were captured for the “Three Point Flexural Bend Test.” The first three specimens tested without the embedded copper foil showed complete fractures with multiple piece separation. The maximum extension was 19.7 mm. The maximum stress was 92.62 MPa. In both specimens with the highest values it can be seen that the breakage was

separated in more than two pieces. From this sample of specimens the average maximum stress was 87.02 MPa with a standard deviation of 7.2 MPa. The graph in **Figure 22** shows that sample 1 and 2 follow a very similar stress strain curve whereas sample 3 had a lower stress versus strain value almost from the beginning. The average strain at failure for the three samples was 0.056 mm/mm with a standard deviation of 0.003 mm/mm. The equation below was used to find the stress for the three point bend test. “F” represented the force applied by the Instron, “L” was the span length; “b” and “d” were the width and thickness of the specimen respectively.

$$\sigma = \frac{3FL}{2bd^2} \text{ [Eqn. 1]}$$

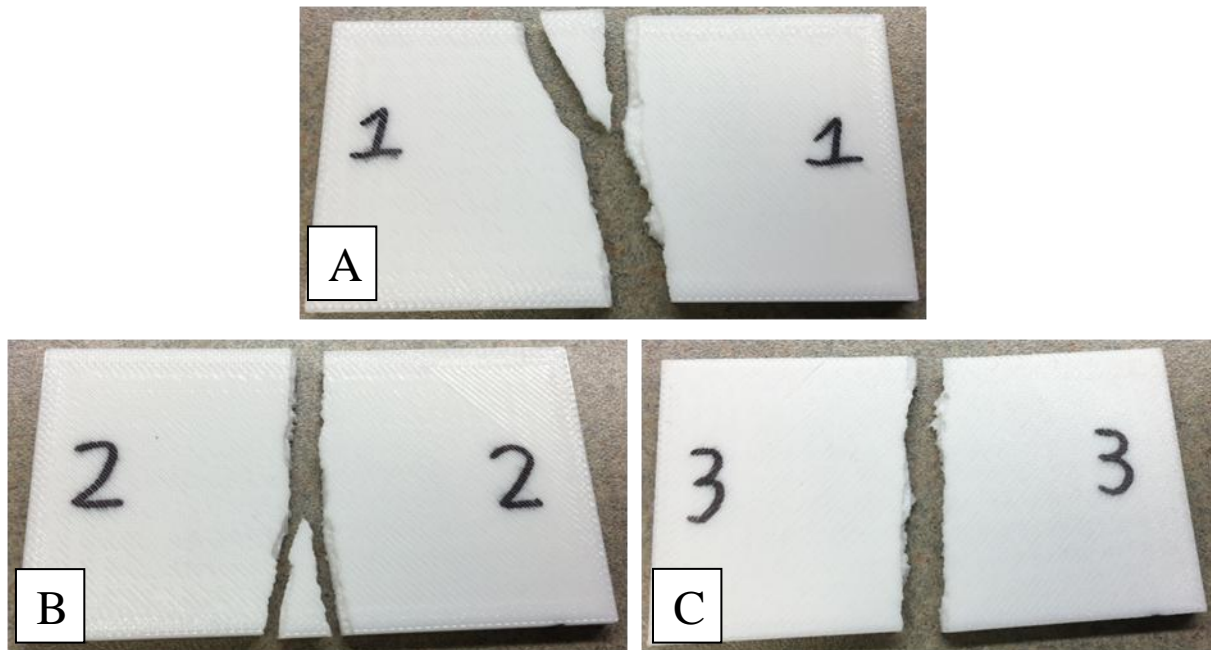


**Figure 21.** Flexural specimens posttest (no foil), A) sample 1, B) sample 2, C) sample 3

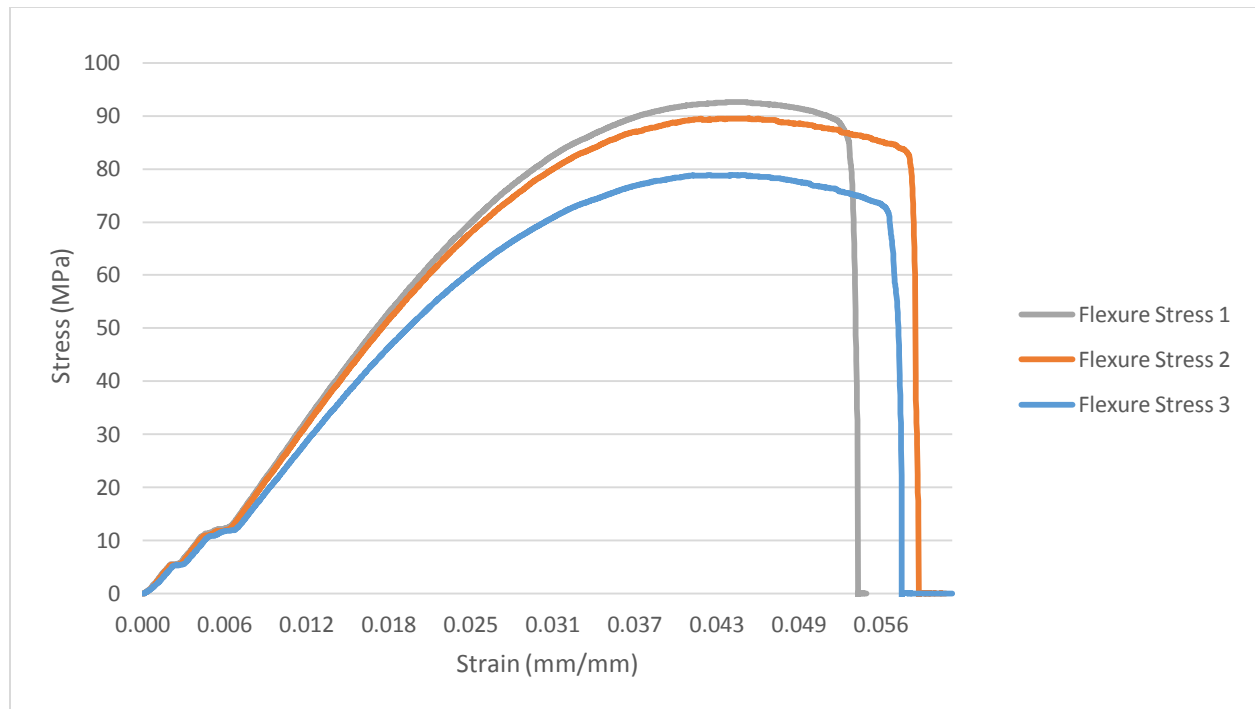


**Figure 22.** Stress Strain graph of no foil specimen for three treatments

The images below show the results of the 12.7 mm foil tests. **Figure 23 A**, shows similar breakage to that of the testing without embedded copper foil. A maintained connection to the broken apart pieces was credited to the copper foil. However, **Figure 23 B** and **C** show a different post test result, these two only cracked along the center. Specimen 2 in **Figure 23 B** only showed cracking at the side with initial cracking developing at 94.9 MPa. As seen in the curve of the graph, the stress dropped but the testing stopped as well. It is assumed that if the test would have continued the curve of sample 2 would have mimicked the curve of sample 1. Specimen three in **Figure 23 C** showed a full crack along the width without separation. Test specimen three in **Figure 23 C** had the highest values for both extension and stress amongst the three samples with an extension of 16.37 mm and a stress of 100.52 MPa. The 12.7 mm foil samples had an average maximum stress of 94.48 MPa with a standard deviation of 5.47 MPa. The samples had adhesive on one side of the foil and ABS solution of the other to adhere the

copper foil to the PC. Although inconclusive, these manually added chemicals could have contributed to the behavior of sample 2 and 3 of the 12.7 mm foil samples. In **Figure 24** the graph shows that all three samples followed the same stress strain curve for more than half of the graph. With the development of an initial crack, both sample 1 and 2 cracked at very close intervals. Sample 3 maintained the stress strain curve for much longer. These results mimicked the way that the samples cracked. The average for strain at break was 0.041 mm/mm with a standard deviation of 0.008 mm/mm. The distributed load that symmetrically broke sample three displayed the best result. The difference in the results could be attributed to the copper foil. The hold on the copper foil to the PC substrate via the adhesive and post process material could be the cause. The application of the chemicals was applied manually and thus could have been applied inconsistently to the three samples. Two chemicals in particular were the adhesive and the ABS solution; both of these solutions purposes were to adhere the copper foil to the PC, one below the copper foil and one above. If the chemicals did not adhere the two materials with full even coverage, due to a lack of application or otherwise, the possibility of the two materials breaking apart under pressure was increased as seen in sample 1.

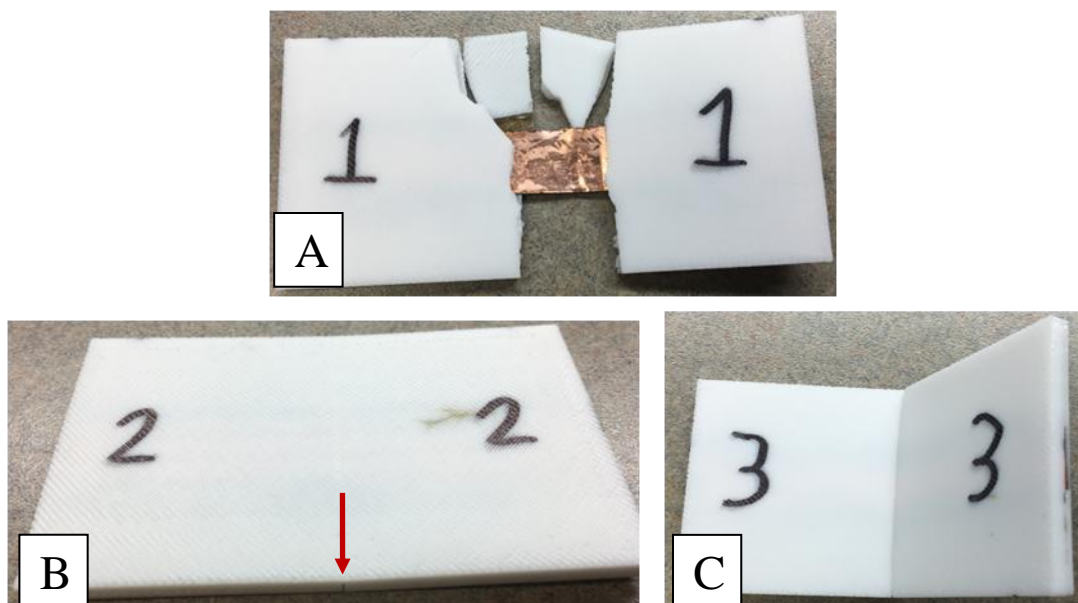


**Figure 23.** Flexural specimens posttest (12.7 mm foil), A) sample 1, B) sample 2 arrow indicates location of fracture, C) sample 3

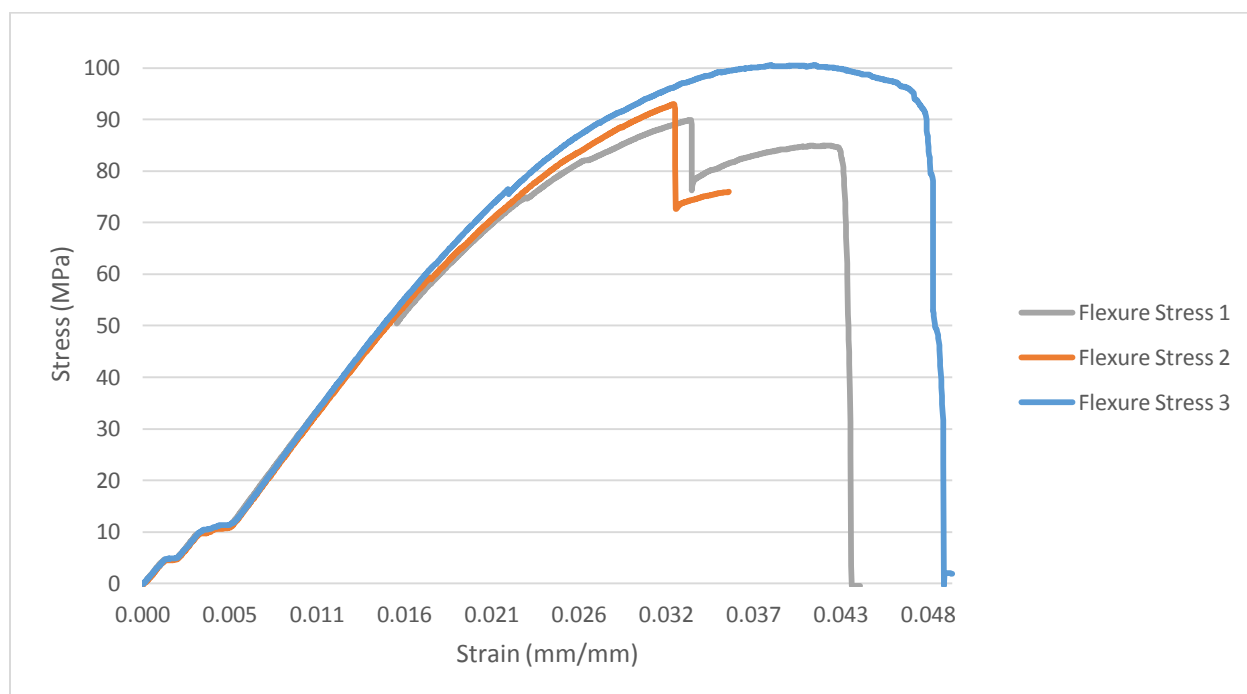


**Figure 24.** Stress Strain Graph of 12.7 mm foil specimen for three treatments

The next three test samples were embedded with 25.4 mm wide copper foil. All of the test specimens in **Figure 25** show that each one broke in a different manner. Specimen four in **Figure 25 A**, not only broke down the middle and separated, but it also split along the face where the foil was applied. The PC effectively slipped off of the copper foil. Specimen five in **Figure 25 B** cracked half way along the width of the test part without any separation. Lastly, specimen six fractured along the width of the part with complete separation similarly to the first tests without embedded copper foil. The largest extension was 12.12 mm. The highest stress was 93.96 MPa. The graph for the stress strain curves for these samples could be seen in **Figure 26** below. The average maximum stress was 86.12 MPa with a standard deviation of 10.66 MPa. As expected from the images of the samples, sample 4 shows a lower stress value. This sample developed an early initial crack and slippage, most likely causing the low stress values. This could be assumed to be a result of inconsistent chemical application for adhesion as in the previous tests. Sample 4 showed complete separation from the front side of the sample while showing the copper foil sliding away from the edge of the back side of the sample. In **Figure 25 A**, the red arrow indicated the location that the edge of the foil strip slipped away from the edge of the substrate. The black arrow shows evidence of good adhesion on the copper foil. The green arrow however, shows evidence of a lack of adhesive on the copper foil. This clean surface is believed to have led to the slippage that occurred between the copper foil and PC.



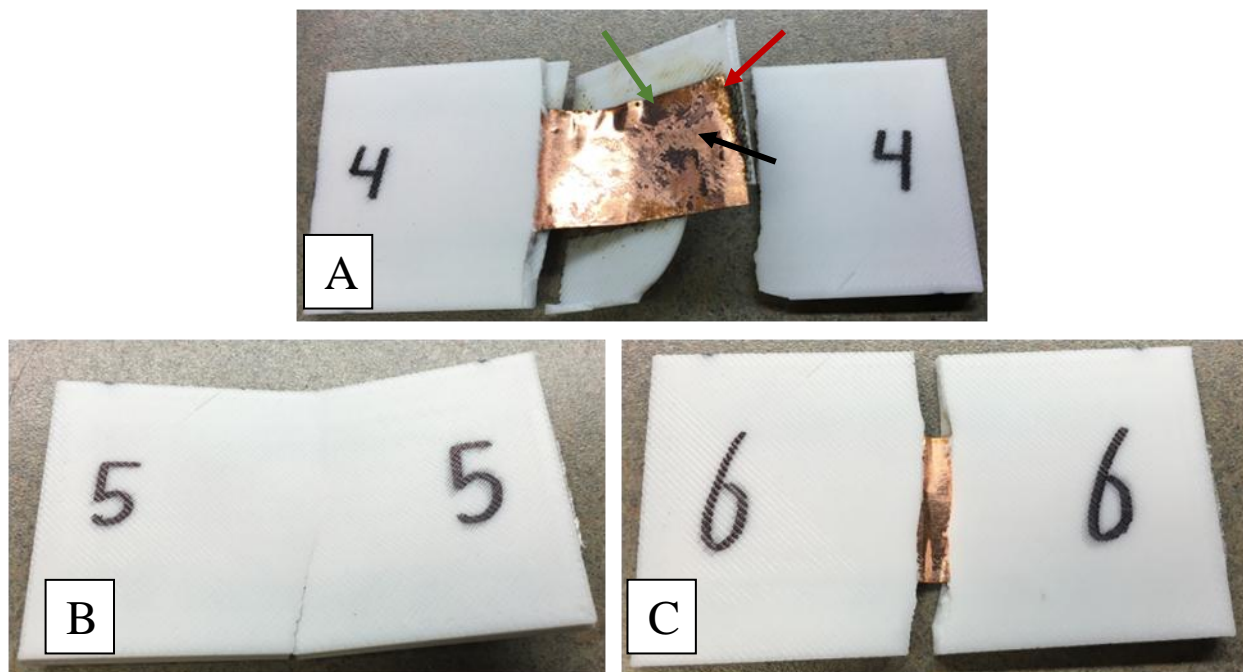


**Figure 25.** Flexural specimens posttest (25.4 mm foil), A) sample 4, B) sample 5, C) sample 6

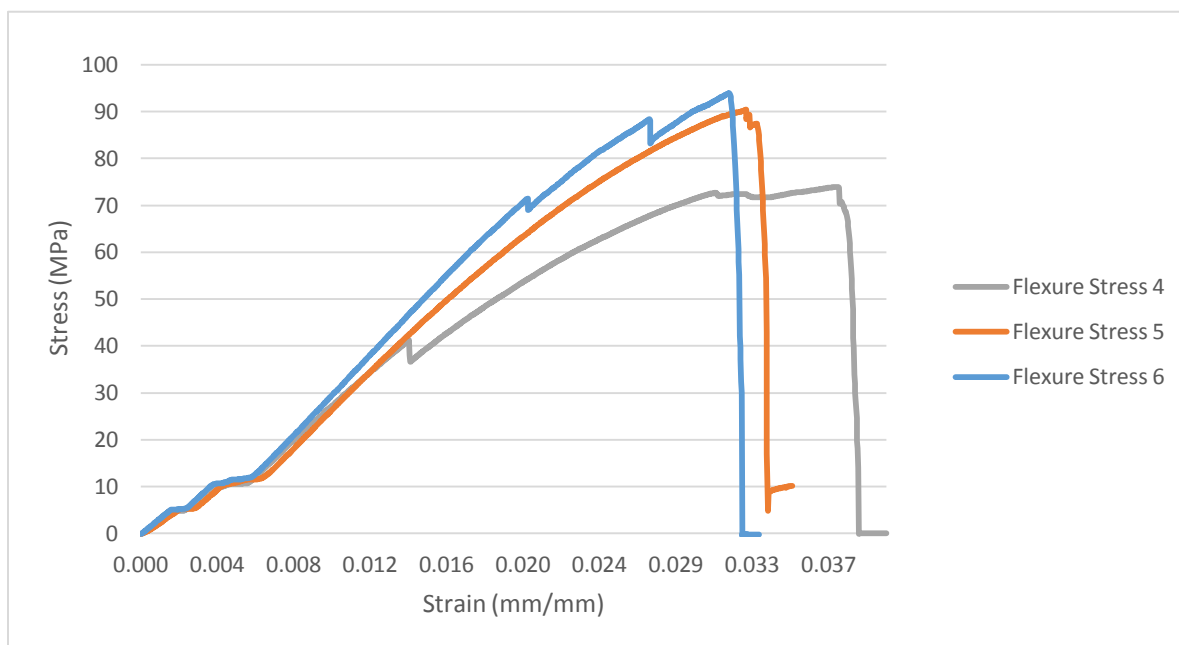


**Figure 26.** Stress Strain graph of 25.4 mm foil specimen for three treatments

The two graphs below **Figure 27** and **Figure 28** show the maximum flexural stress for the three treatments and the flexural extension at break for the three treatments respectively. Each of the points on both graphs were the average of three measurements using standard deviation to create the error bars. The samples with the 12.7 mm foil were the best overall. The flexural stress graph of the three treatments showed inconsistent results due to inconsistencies in the manual application of the multiple adhesive chemicals. The 25.4 mm foil that had similar results to the samples without foil. For the maximum flexural stress the percent difference between the specimens with no foil and the ones with 12.7mm foil was a 8% increase. The difference between no foil and 25.4 mm foil was -1%. However, the range of values seen in the treatment with 25.4 mm foil was greater than the range of the treatment with no foil. The slippage that occurred in sample 4 of the 25.4 mm copper foil specimen caused the values in the maximum flexural stress graph to drop. It is assumed that if the application of adhesive chemicals was automated the maximum flexural stress would have increased with the width of the copper foil.

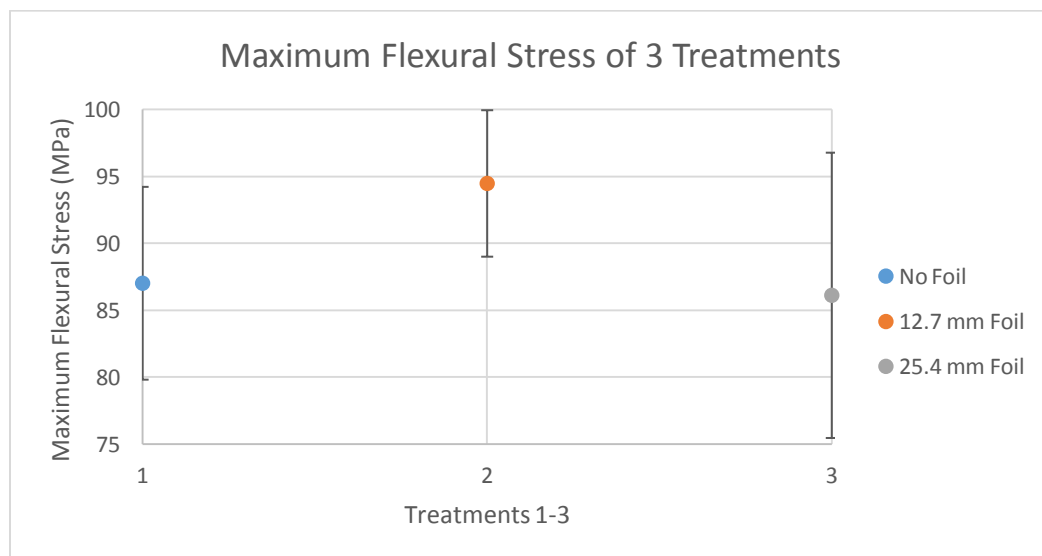


**Figure 27. Maximum Flexural Stress** graph of three treatments

The width of the copper foil had a direct correlation to the flexural extension at break. The wider the foil, the lower the extension. The trend of the three treatments was a seemingly linear trend and with the automated application of the adhesives it is predicted that the trend will remain the same. The percent difference in flexural extension between the samples without foil and of those with the 12.7 mm copper foil was -19%. The percent difference between no foil and 25.4 mm foil was -42%.

12.7 mm foil had the higher flexural strength because of a smaller surface area of copper foil for the application of adhesive and ABS solution that kept the plastic together. 25.4 mm foil had multiple cracks before breaking that could be caused from the larger amount of foil and was slipping away from the plastic. Although inconsistent due to manual applications of chemicals, the inclusion of copper foil into the PC samples showed an increase of the flexural stress. The variability noted in the fracture of samples with foil are all the more reason to fully automate the FA tool.

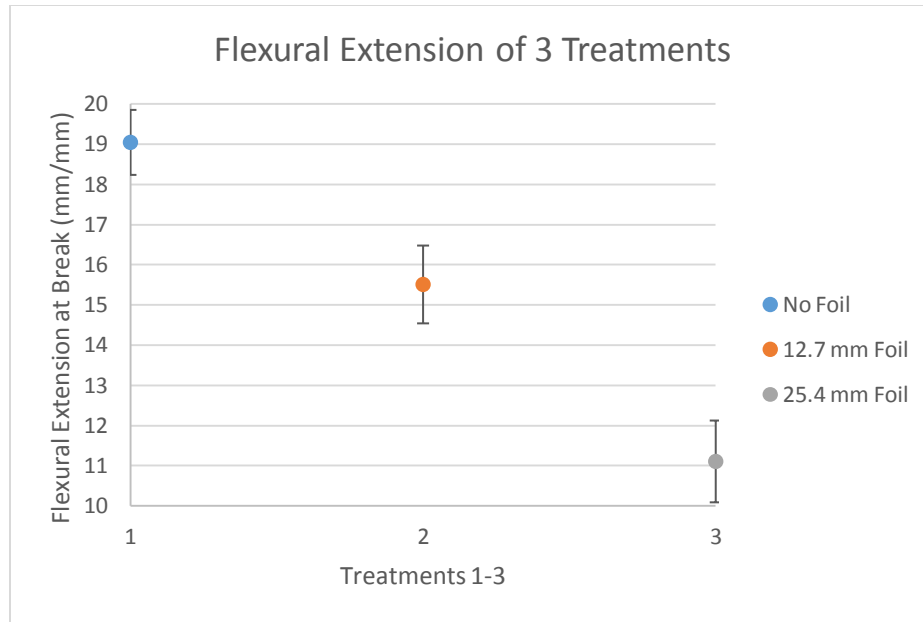


**Figure 28.** Flexural Extension graph of three treatments

The next test was the “Straightness Test”. The photos in **Figure 29** show the direction the copper foil was applied, denoted by the direction of the black arrows. All five specimens were replicates with similar treatments. The graph in **Figure 30** shows data collected from Part 1. The measurement difference depicted in the graph was measured from the target value distance of 12.7 mm from the edge of the PC substrate to the copper foil on both the left and right side.

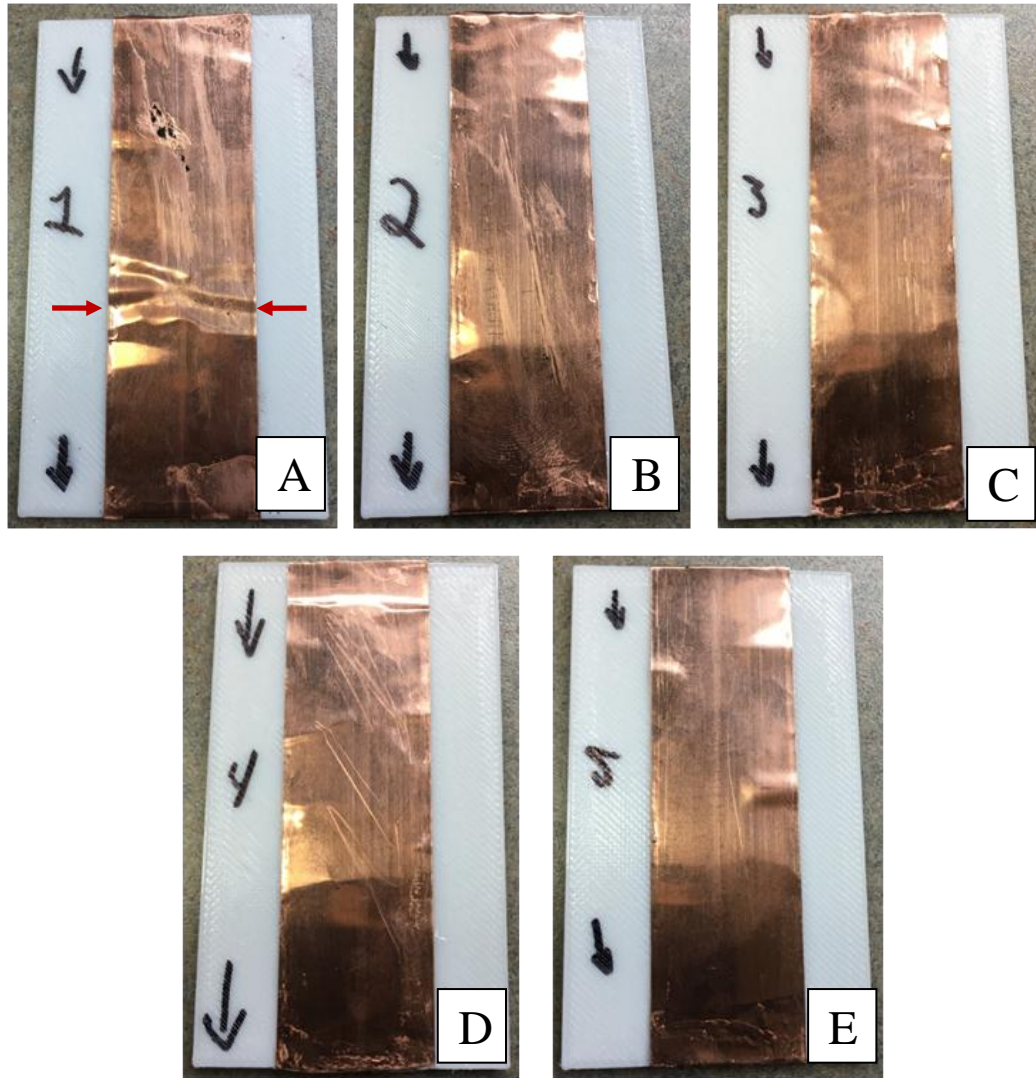


**Figure 29.** Test of straightness specimens A) part 1 arrow indicates wrinkle of foil, B) part 2, C) part 3, D) part 4, E) part 5

The graph was oriented in relation to the test specimen at a 90° turn counterclockwise. The numbers to the left most side of the graph depicted the measurements for the bottom of the test specimen and the right most side of the graph are the top. The purpose of this test was to determine how accurately the FA tool applied the copper foil along the length of the substrate. In **Figure 29** above A, B, C, D and E represent part 1, 2, 3, 4, and 5 respectively.

All the data was taken using the optical gaging products (OGP) smart scope measurement. The next two tests included measurements of distances between the applied foil as well as accuracy of where it was applied with respect to the datum. The goal of these tests were to test repeatability, resulting in a collection of data. The data exhibited how accurately the FA tool could apply foil onto a substrate relative to the edge.

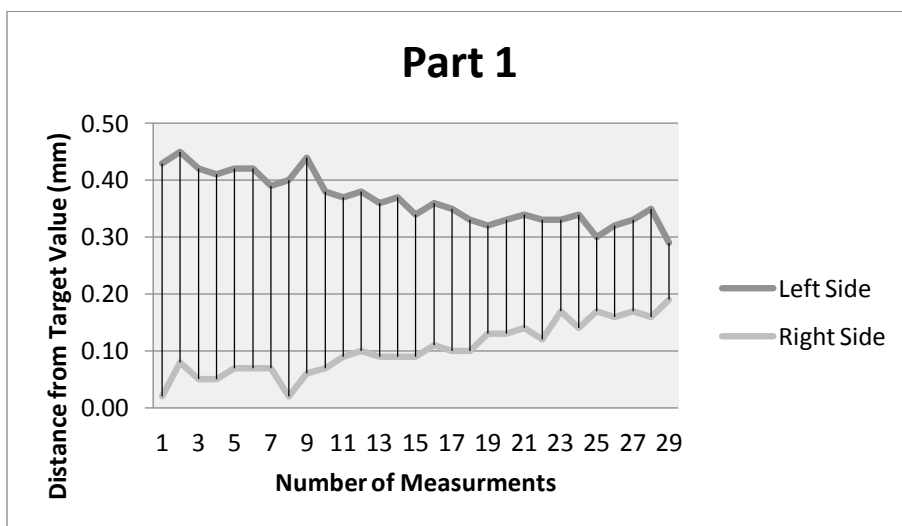


**Figure 30.** Graph of change in distance from foil to the edge of substrate (Part 1)

The results for part one appeared symmetrical on either side of the copper foil with respect to the PC part's edge. The spike at measurement eight and nine could be seen in the image of the test piece denoted by the red arrows, where the foil wrinkled across its width. Parts 2 through 5, although not as symmetrical as the results for part one, each displayed a different result and most of the changes in the graphs could be related to the texture of the foil. The graph in **Figure 31** shows the results of all five specimens of the "Straightness Test". The maximum, median and minimum values were shown with the boxes. The error bars represent the difference between the maximum and third quartile for the top and the difference between the first quartile and the minimum for the bottom. These samples were applied with the copper foil using the FA

tool but were centered on the substrate manually. Thus producing sample parts that were not perfectly centered. The point of this test was not to hit the target value but to show the similarities in the range to determine how straight the foil was applied by the FA tool. In **Figure 29** Part 4 appears to have one of the smoother surfaces of the five samples with minimal wrinkles in the foil. However, in the box plot below Part 4 had the largest values both in distance from the target value and in the range of its values. These results lead to the assumption that the surface texture of the copper foil does not necessarily correspond with the straightness of the sample. The variation in the difference of the range could most likely be due to the small leeway of space, a clearance of 1 mm in the guide to allow for the copper foil to be pulled through with the roller with minimal friction from rubbing against the inside walls of the guide.

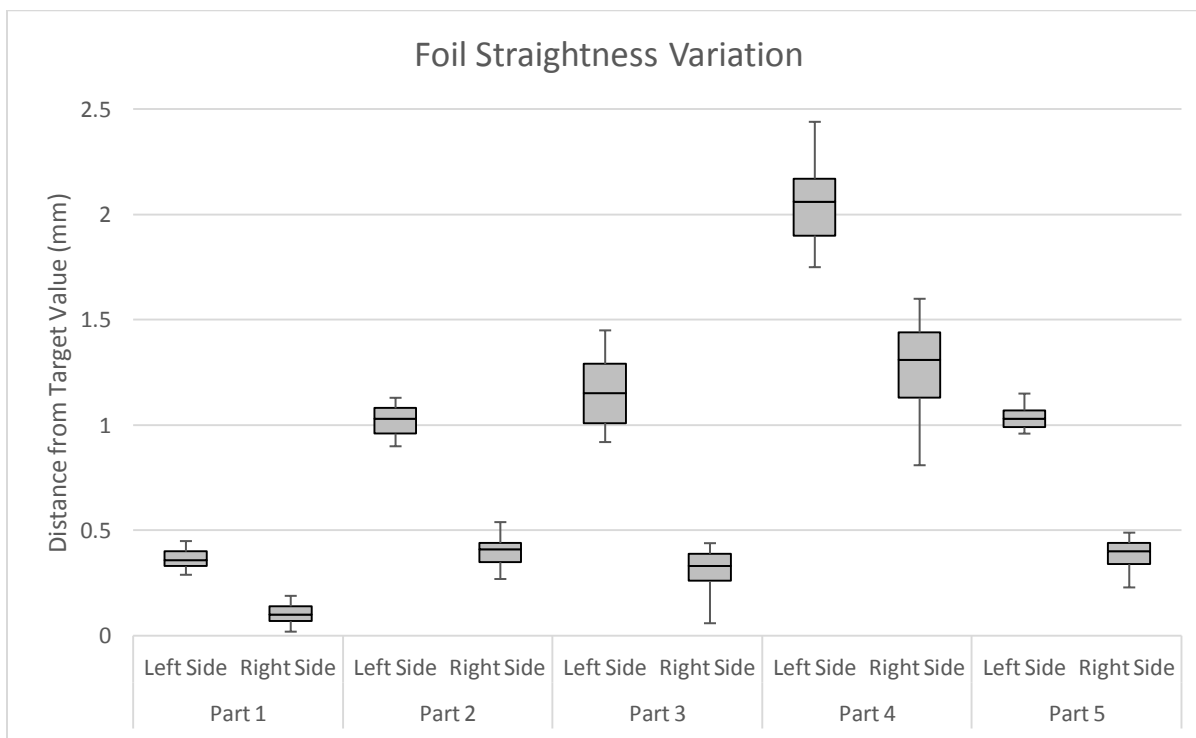


**Figure 31.** Straightness test box plot for measurements from edge of five specimens

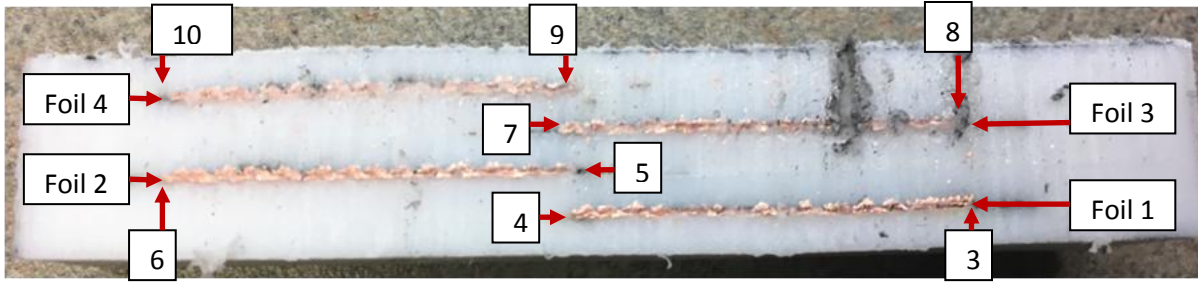


**Figure 32.** Slice 4 of the four layer embedded sample

The following experiment tested the repeatability of the FA tools capability to apply copper foil to the same spot multiple times. **Figure 32** above shows Slice 4 of the five slices. Using the OGP, ten individual measurements were taken along the length of each of the foils. The measurements taken show the difference in height across their length. It was important to know these measurements because the distance between the embedded ground planes and radiating elements were critical. Knowing how smooth the foil was applied helps to understand what changes could be made, if needed to create a smoother embedded foil. The graph in **Figure 33** showed the ten measurements for each foil in Slice 4. The hollow circles depicted by the “0” value in the legend show what the expected values should be. 4.1 - 4.4 in the legend of the graph below indicate the slice and foil number respectively. The first digit (4) represents the slice number and the number after the decimal (1 – 4) represent the foil number referenced in **Figure 32**.



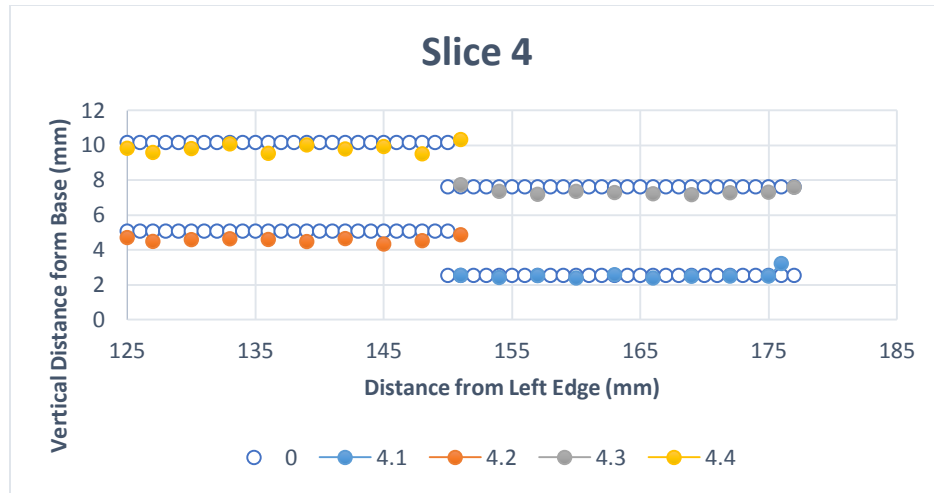


**Figure 33.** Graph of slice 4 of the four layer embedded sample, hollow circles indicate expected values, and solid circles indicate actual values (the numbering of each series as per the next example)

Aside from the ends on either side of the four foils, the lines were very close to straight. All of the ends were slightly upward from the rest of the foil. The percent error for the points at the edge of the foil were larger than those closer to the center. For future evaluation an alternative of a CT scan could be used to measure the embedded foil without cutting the sample. The foils that were applied in the PC part were paused so that the copper would be applied at every 2.54 mm in the “z” direction. Meaning that the distance in between each of the foils would be 2.54 mm. From the bottom of the test part the first pause would be Foil 1 at 2.54 mm, then Foil 2 at 5.08 mm, next Foil 3 at 7.62 mm and the last pause for Foil 4 at 10.16 mm, measurements taken from the bottom of the specimen.



**Figure 34.** Warped test substrate

Foils 1-3 did not display a true characterization of the process. The data was misrepresented due to multiple reasons: initially the print of the substrate was warped during the printing process, leading to the misalignment of the embedded foils 1 and 3 as seen in **Figure 34**. The roughness in the cutting technique was another factor that affected the data. It is the author's opinion that Foil 4 best characterized the data for this test due to its lack of warping. All the values in **Table 4.1** were percentages representing the data from Foil 4 in all five slices. The averages were calculated using the absolute value of the percent difference. Given the maximum percent difference observed the FA tool can place the copper foil within 8% of the required value along the "z" height.

**Table 4.1** Foil 4 averages for all five slices

Averages	Slice 1	Slice 2	Slice 3	Slice 4	Slice 5
Foil 4	7.5	1.7	5.0	3.5	3.1

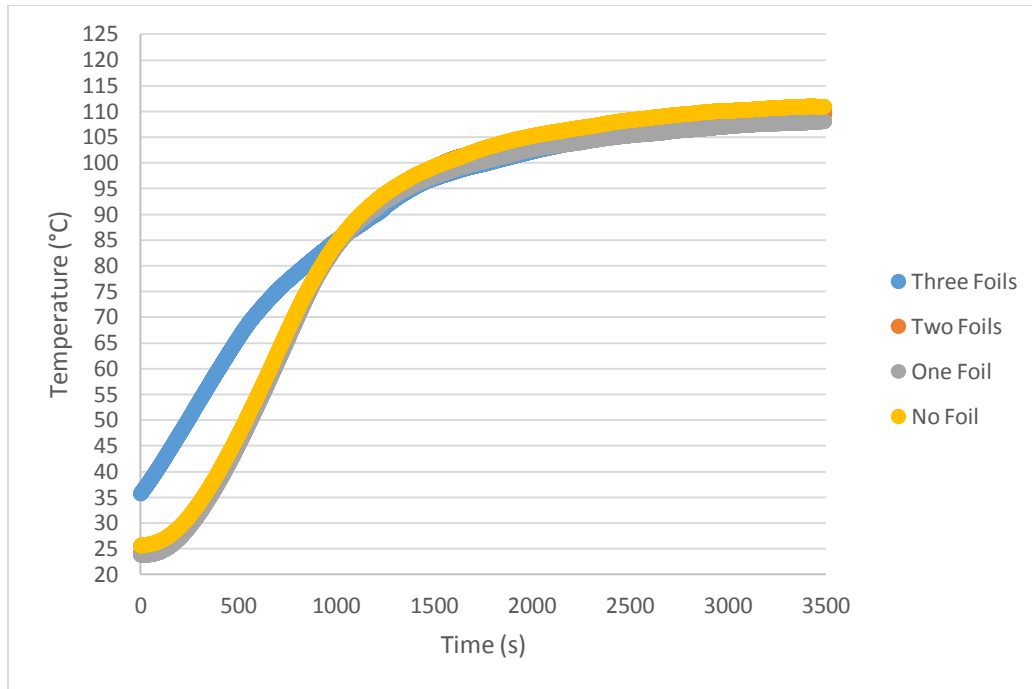


**Figure 35.** Graph of heat transfer at measurement 1 (note that the series No Foil, One Foil and Two Foils were similar and as such the Two Foils series was unobservable in the chart)

The last test done was the “Heat Transfer Test.” The graph above in **Figure 35** shows the results of the four test specimens after one hour. Measurement 1 was representative of the first of five thermocouples in each strip. Each measurement taken from all four specimens was from side 1, the face touching the heat source. These temperatures represented the highest readings from the test. As seen in the graph above all four specimens included the one without any foil reached approximately the same temperature at the end of the hour.

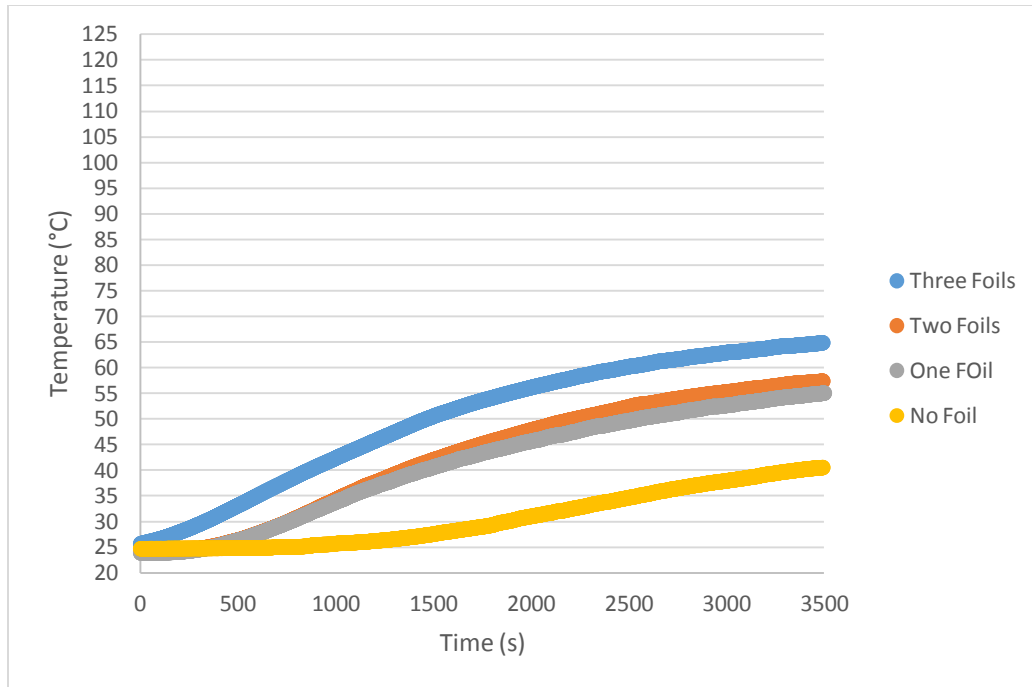


**Figure 36.** Graph of heat transfer at measurement 5

At the opposite side of the heat transfer part however the results differed. Measurement 5 shown in the graph in **Figure 36** above was representative of the fifth measurement in each strip of the four test specimens. This thermocouple was placed on side 3, the spot furthest from the heat source. These results exhibited how much of the heat was transferred from one side of the test specimen to the other. The part with One Foil showed a 26.3 percent increase in temperature compared with the test pieces that had No Foil and the percent difference from Three Foils to the No Foil specimen was a 37.5 percent increase. However, one foil and two foil specimens showed very similar curves with a percent difference of 4.1 percent. The percent increase between Two Foils and Three Foils was 11.5 percent. The test piece with three foils reached the height of the One Foil specimen at 55°C in 2000 seconds versus the full time it took for One Foil to reach that temperature (3500 seconds).

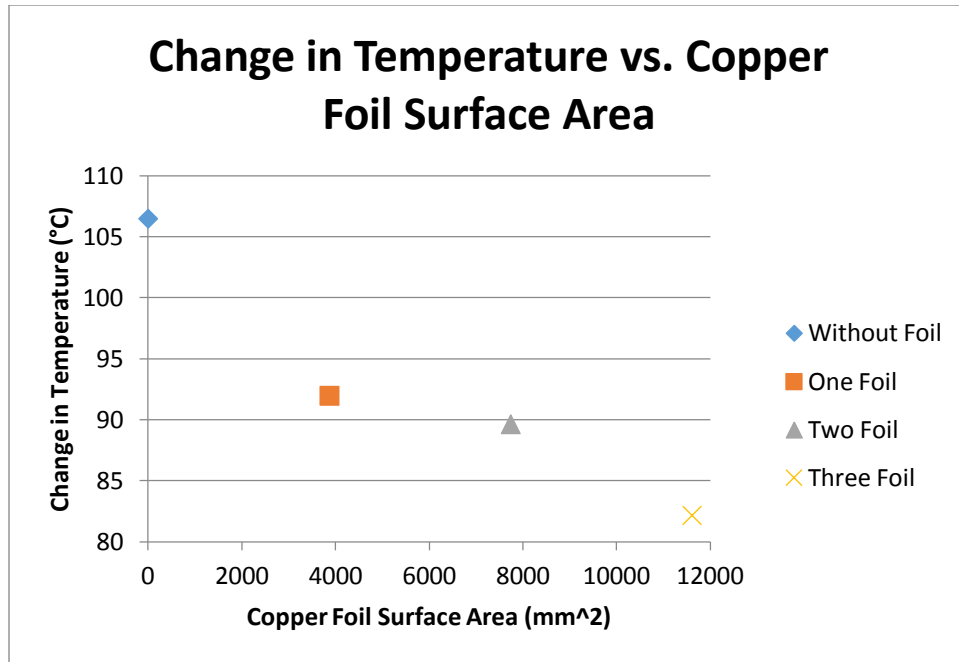


**Figure 37.** Graph of the change in temperature across one foil vs. the change in surface area

The reason for test piece One and Two Foil being so similar could perhaps be explained with the data from the graph above in **Figure 37**. The change in temperature shown in the graph was calculated by subtracting the temperature of the heating plate (147°C) to the final temperature of measurement 5 on side 3. This temperature change showed a direct correlation with an increase in surface area. Ideally, the less of a temperature change meant that there was a high amount of heat transfer across the foils. The small intervals of the values of One and Two Foil in **Figure 35** and **Figure 36** could be related to the distance between the foils. The specimen with two strips were placed on the left and right side of the part, a considerable distance between them, enough so that conducting heat from one foil could not affect the other. This was similar to the test part with one foil, there was no other foil affecting the heat transfer of the strip. Whereas the part with three strips were closer together and were more likely to transfer

the heat not only along the strips but also across one copper foil strip to another via heat transfer through the PC.

## **CHAPTER 5**

### **CONCLUSION AND FUTURE WORK**

#### **5.1 Conclusion**

The FA tool underwent two different designs, the first fulfilled all of the requirements except for size, and the second design adjusted all of the features to fit all of the requirements and made the tool easier to maintenance. Design one of the FA tool featured individual plates for each of the components. A gear box motor was added to rotate the pinch rollers but had too low of a torque (14.7 Kg-cm) to overcome the resistance of the copper foil spool. Also, a copper foil spool with dimensions equal to the width requirement of the tool (127 mm) was mounted at the top of the FA tool. Design two of the FA tool remedied these problems. The 12 plates were minimized to seven, allowing for fewer bolts and easier access to the components. The motor was changed to a stronger motor (20.9 Kg-cm) and was able to overcome the friction of the copper foil spool at a low speed of 4 RPM. Lastly the copper foil spool was reduced to so that the new OD was smaller than the original ID. These changes along with others made to the FA tool in design two created a tool that was within the design constraints of the tool while making it functional and operable.

The experiments that were done, resulted in various findings with the application of foil using the FA tool with printed substrates. Four different assessments were done, all of which resulted in different findings of the application of embedded foil. The first test applied copper foil to a substrate for the purpose of testing the flexural strength to samples with and without copper foil. The result was a direct correlation of a decrease in flexural extension to an increase in the width of copper foil. Although an automated system was not tested, it is assumed that with

the incorporation of an automated adhesive application process, the increase in width of the copper foil would also increase the flexural stress values in a linear trend. The percent difference of the maximum flexural stress between the specimens with no foil and the ones with 12.7mm foil was an 8% increase. The difference between no foil and 25.4 mm foil was -1%. The “Straightness Test” provided positive results in the horizontal displacement of an embedded copper foil with a maximum displacement of 0.4 mm on either side of the foil. The third experiment tested the accuracy of placing the foil in the same position repeatedly in a “Z” height direction. The FA tool applied the foil repeatedly in the designated position within 8% of the desired location. The fourth and final experiment tested if the application of foil to a part would improve the heat distribution. One, two and three copper foil strips were applied along three faces of a PC block and then placed one of the exposed sides of the copper onto a heating plate. Thermocouples were strategically placed to determine the heat transfer across the PC part. There was an increase of change in temperature of the copper foil with an increase of copper foil surface area with a difference in temperature ranging from 106°C for the no foil specimen to 82°C for the three foil specimen with a percent difference of 23 percent.

The FA tool showed promising results for embedding copper foil. Testing of the tool’s operation through various testing procedures produced results under a ten percent error in foil placement. The results also showed that the embedded copper foil through the application of the FA tool created parts with automated processes that had multiple purposes, such as structural purposes or thermal dissipation. Overall, the FA tool had shown big improvements to the HM process and more doors will open in the future to different types of systems that could contribute more than one process within a solitary machine. With all the developments of this tool and its



intended incorporation into the Multi<sup>3D</sup> Manufacturing System, the future of additive manufacturing will continue to grow.

## **5.2 Future Work**

The ultimate goal of the FA tool was to create a fully automated tool to embed copper foil without the help of human interaction. Future work to be considered to further improve the FA tool included the installation of an automated cutting system. The tool required the copper foil to be cut manually after the application process was complete to separate the applied foil from the roll of foil attached to the tool. To automate the tool, applying the adhesive automatically would be a beneficial aspect of the FA tool. Although not incorporated into the FA tool, a prototype of the adhesive dispenser was created. Future work of the tool could entail attaching the dispenser and testing it for use in the application of the copper foil. Another important addition to the tool would be to use Teflon or another similar insulator to separate the upper and lower parts of the FA tool, therefore only exposing the roller below to the 200°C printing envelope with minimal heat traveling through the guide and into the upper part of the tool. Doing so would allow for the pinch rollers, motor and all other heat sensitive components the capability of being used in the FA tool. Otherwise heat resistant materials would need to replace them, raising the cost of the tool. An example is the application roller; the roller mounted on the FA tool has an operating temperature of 176<sup>0</sup>C and was \$77.96. The roller rated 24 degrees higher at an operating temperature of 200<sup>0</sup>C was \$337.19.

Although not tested, the FA tool had the capability of applying different thicknesses and widths of copper foil. There was a specific range to the width and thickness of the foil that could be used to accommodate the width of the roller as well as the “z” height tolerance of the 3D

printer that could be tested. In the results of the heat transfer test, the test specimens with One and Two Foils exhibited very similar heat distribution. It was recommended that further testing should be done where the two foils would be applied onto the heat transfer part multiple times, each time the two foils gradually getting closer to the center. It was expected that the closer the foils got to one another, the temperature difference would become more similar to that of the specimen with three foils. Another test that should be conducted is a surface roughness test. After the application of the copper foil onto a substrate of a user defined length no subsequent layers should be printed. The roughness found on the surface could be the result of the distribution of the adhesive and the roller application. Results from this test could be related with patch antenna ground plane readings. Testing should also be done using the FA tool to apply copper foil onto substrates with sloped surfaces or otherwise complex patterns. The capabilities of the coding involved in automating the application using the FA tool and cutting with the CNC led to the belief that successful embedding could be accomplished on complex printed patterns.

## REFERENCES

Aguilera, Efrain, Jorge Ramos, David Espalin, Fernando Cedillos, Dan Muse, Ryan Wicker, and Eric MacDonald. *3D Printing of Electro Mechanical Systems*. Rep. N.p.: n.p., n.d. 2013. Print.

"AM Basics | Additive Manufacturing (AM)." *Additive Manufacturing AM*. N.p., n.d. Web. 20 Sept. 2016.

Ambriz, Steven Daniel. *DESIGN AND DEVELOPMENT OF THE PORTABLE BUILD PLATFORM AND HEATED TRAVEL ENVELOPE FOR THE MULTI3D MANUFACTURING SYSTEM*. Thesis. W.M. Keck Center for 3D Innovation, 2015. N.p.: n.p., n.d. Print.

Bak, David. "Rapid prototyping or rapid production? 3D printing processes move industry towards the latter", *Assembly Automation*, Vol. 23 Iss: 4, pp.340 – 345, 2004. Print.

Caffery, Tim, Terry Wholers, and Ian Campbell. *Wholers Report 2016*. Fort Collins: Wholers Associates, Inc., 11 July 2016. PDF.

"Cooling 101: The Basics of Heat Transfer." *Cooling 101: The Basics of Heat Transfer*. N.p., n.d. Web. 03 Oct. 2016.

Ghosh, Arun, and David A. Schiraldi. *Improving Interfacial Adhesion between Thermoplastic Polyurethane and Copper Foil Using Amino Carboxylic Acids*. Rep. N.p.: n.p., n.d. 2009. Print.

Hochstettler, Spencer. "Rust Removal Using Electrolysis." *Rust Removal Using Electrolysis*. N.p., 1998. Web. 05 Jan. 2017.

"How FDM 3D Printing Works." *FDM Technology, About Fused Deposition Modeling*. N.p., n.d. Web. 20 Sept. 2016.

Huske, M., J. Kickelhain, J. Muller, and G. EBer. *Laser Supported Activation and Additive Metallization of Thermoplastics for 3D-Mids*. Rep. N.p.: n.p., n.d. 2001. Print.

"Hybrid Metal Manufacturing -a Core Application for Optomec Additive Manufacturing Solutions." *Optomec*. N.p., n.d. Web. 14 Dec. 2016.

Keating, Steven, and Neri Oxman. "Compound Fabrication: A Multi-functional Robotic Platform for Digital Design and Fabrication." *Robotics and Computer-Integrated Manufacturing* 29.6 (2013): 439-48. Web. 26 Feb. 2017.

Kurman, Melba, and Hod Lipson. *Fabricated: The New World of 3D Printing*. N.p.: Wiley, 2013. Print.

Lopes, Amit Joe, Eric Macdonald, and Ryan B. Wicker. "Integrating Stereolithography and Direct Print Technologies for 3D Structural Electronics Fabrication." *Rapid Prototyping Journal* 18.2 (2012): 129-43. Web.

Maier, Karyn. "What Is Thermoplastic." *WiseGeek*. Ed. Bronwyn Harris. Conjecture, 29 Aug. 2016. Web. 21 Sept. 2016.

Marquez, Daniel Abraham. *DEVELOPMENT OF THE THERMAL WIRE EMBEDDING TECHNOLOGY FOR ELECTRONIC AND MECHANICAL APPLICATIONS ON FDMPRINTED PARTS*. Thesis. The University of Texas at El Paso, n.d. N.p.: n.p., n.d. 2016. Print.

Maxey, Kyle. "A Profile of Hybrid Additive Manufacturing Technology." *Engineering.com*. N.p., 5 Aug. 2015. Web. 20 Sept. 2016.

Metals, Online. "0.005" C110 COPPER FOIL." Order Copper 110 Foil in Small Quantities at OnlineMetals.com. N.p., n.d. Web. 08 Oct. 2016.

Nagel, Jacquelyn K. S., and Frank W. "Hybrid Manufacturing System Design and Development." *Manufacturing System* (2012): n. pag. Web. 26 Feb. 2017.

Nelson, Norvell J. Copper Etching Process and Solution. Psi Star, assignee. Patent US4632727 A. 30 Dec. 1986. Print.

Palermo, Elizabeth. "Fused Deposition Modeling: Most Common 3D Printing Method." *LiveScience*. Purch, 19 Sept. 2013. Web. 05 Jan. 2017.

Priedeman, William R., Jr. Process of Making a Three-dimensional Object. Stratasys, Inc., assignee. Patent US6645412 B2. 11 Nov. 2003. Print.

ServicesStereolithography Selective Laser Sintering PolyJet 3D Printing Fused Deposition Modeling Urethane Castings Metal PrototypingLearning CenterNews Rapid Prototyping Blog Case Studies White Papers How Tos Ask ProtoMANContactAbout Videos Finish Levels. "The History of Additive Manufacturing | ProtoCAM." *ProtoCAM*. N.p., 20 Nov. 2015. Web. 21 Sept. 2016.

Shemelya, Corey, Fernando Cedillos, Efrian Aguilera, David Espalin, Danny Muse, Ryan Wicker, and Eric Macdonald. "Encapsulated Copper Wire and Copper Mesh Capacitive Sensing for 3-D Printing Applications." *IEEE Sensors J. IEEE Sensors Journal* 15.2 (2015): 1280-286. Web.

Shemelya, Corey, Mike Zemba, Min Liang, Xiaoju Yu, David Espalin, Ryan Wicker, Hao Xin, and Eric Macdonald. "Multi-layer Archimedean Spiral Antenna Fabricated Using Polymer Extrusion 3D Printing." *Microwave and Optical Technology Letters* 58.7 (2016): 1662-666. Web.

Sher, Davide. "The 10 Fastest 3D Printers in the World." *All3DP*. N.p., 05 Feb. 2016. Web. 03 Jan. 2017.

"The 7 Categories of Additive Manufacturing | Additive Manufacturing Research Group | Loughborough University." *The 7 Categories of Additive Manufacturing | Additive Manufacturing Research Group | Loughborough University*. N.p., n.d. Web. 26 Nov. 2016.

Yamanishi, Keisuke, Hideo Oshima, and Kazuhiko Sakaguchi. Copper Foil for Printed Circuits and Process for Producing the Same. Nikko Gould Foil Co., Ltd., assignee. Patent US 5366814 A. 22 Nov. 1994. Print.

Yates, C., and A. Wolski. Copper Foil Treatment and Products Produced Therefrom. Yates Industries, assignee. Patent US3857681 A. 31 Dec. 1974. Print.

Yusuf, Bulent. "35 Challenging Dual Extruder 3D Printer Models (for Free)." *All3DP*. N.p., 22 Oct. 2016. Web. 2 Jan. 2017.

Zhu, Z., V. G. Dhokia, A. Nassehi, and S. T. Newman. "A Review of Hybrid Manufacturing Processes – State of the Art and Future Perspectives." (2013): 596-615. Web. 26 Feb. 2017.

## APPENDIX

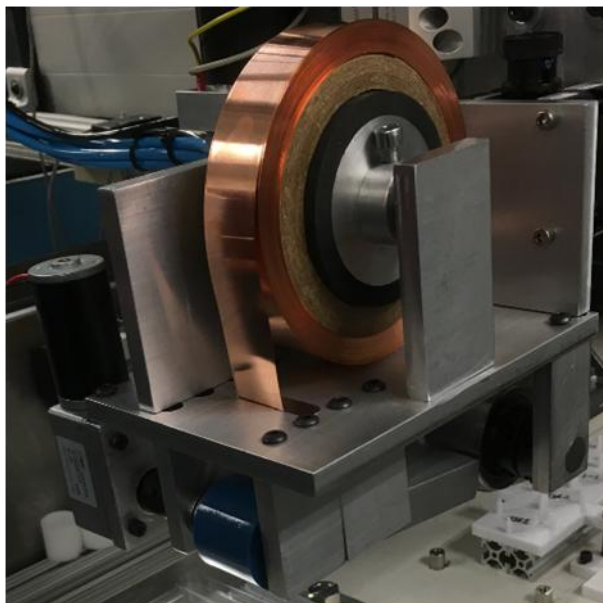


**Figure 38.** First design of FA Tool

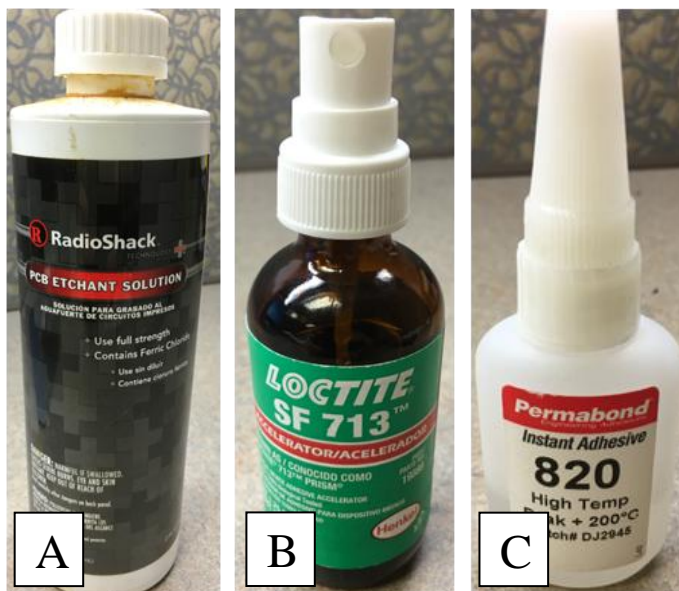


**Figure 39.** A) Etchant, B) accelerant, C) adhesive



**Figure 40.** Sample 5 of flexural testing in the Instron



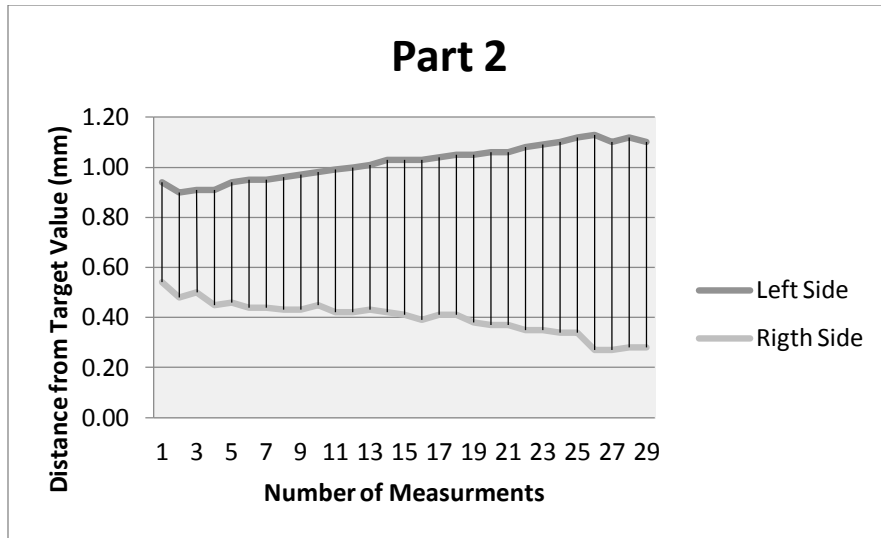


**Figure 41.** Graph of change in distance from foil to the edge of substrate (Part 2)

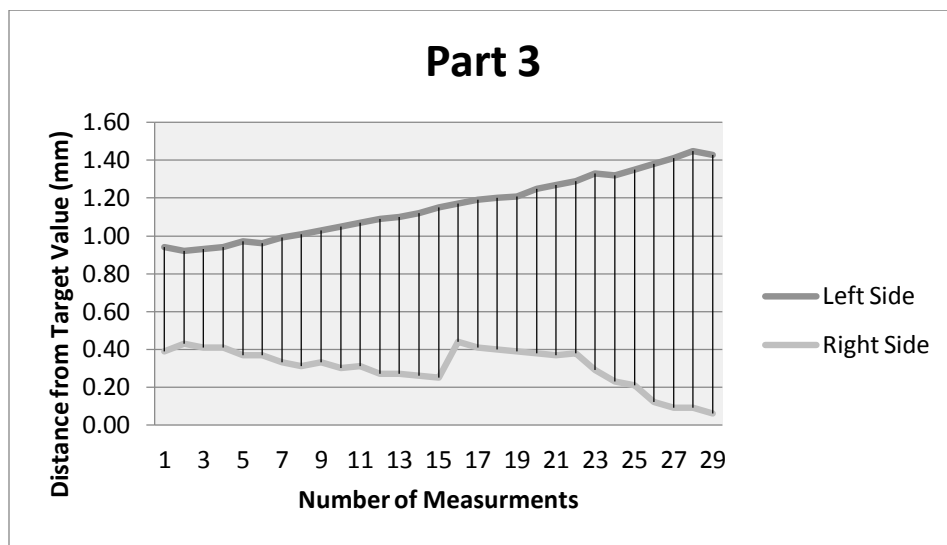


**Figure 42.** Graph of change in distance from foil to the edge of substrate (Part 3)

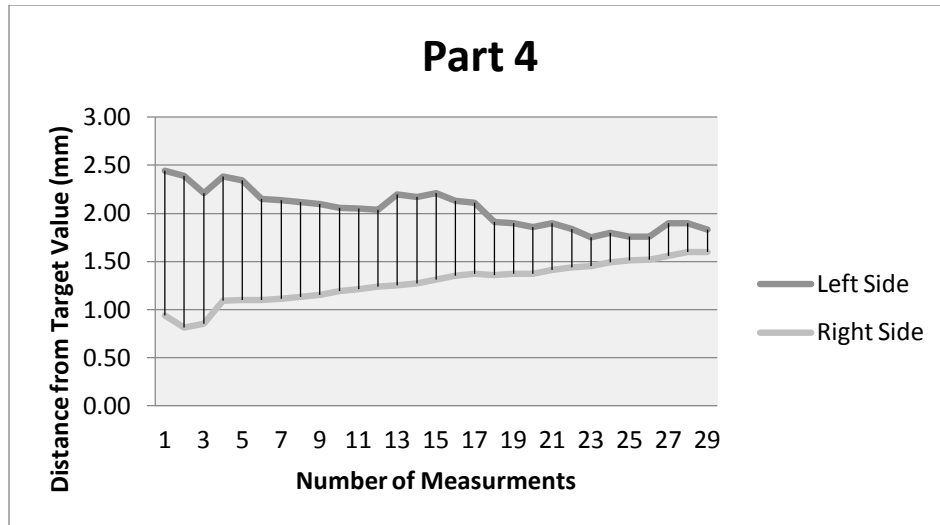


**Figure 43.** Graph of change in distance from foil to the edge of substrate (Part 4)

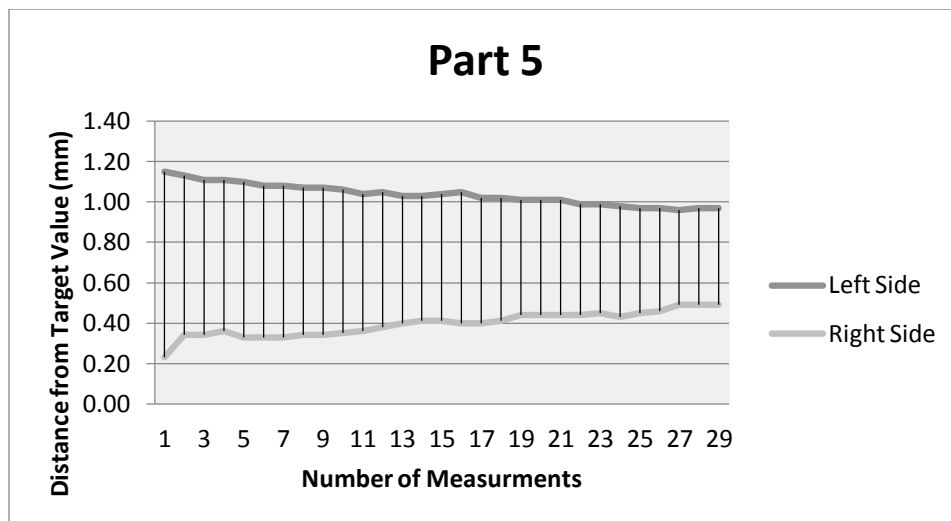


**Figure 44.** Graph of change in distance from foil to the edge of substrate (Part 5)



**Figure 45.** OGP measuring slice 5 of the four layer embedded sample

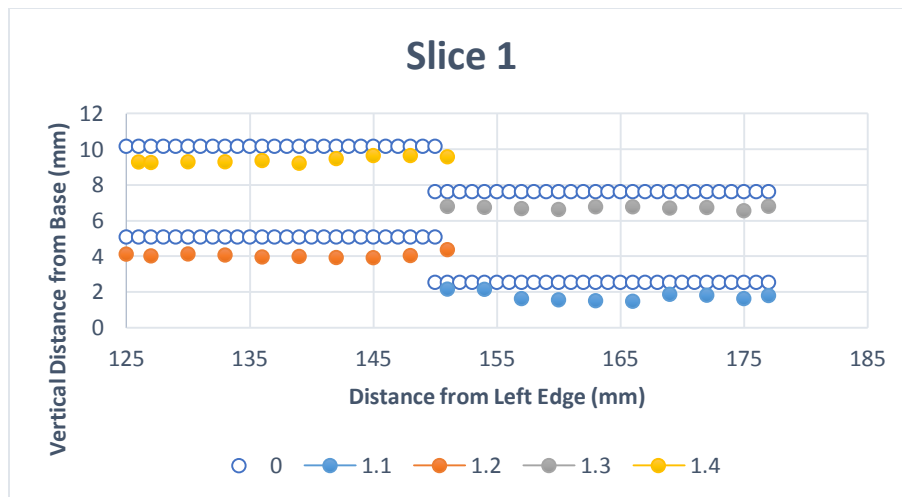


**Figure 46.** Graph of slice 1 of the four layer embedded sample

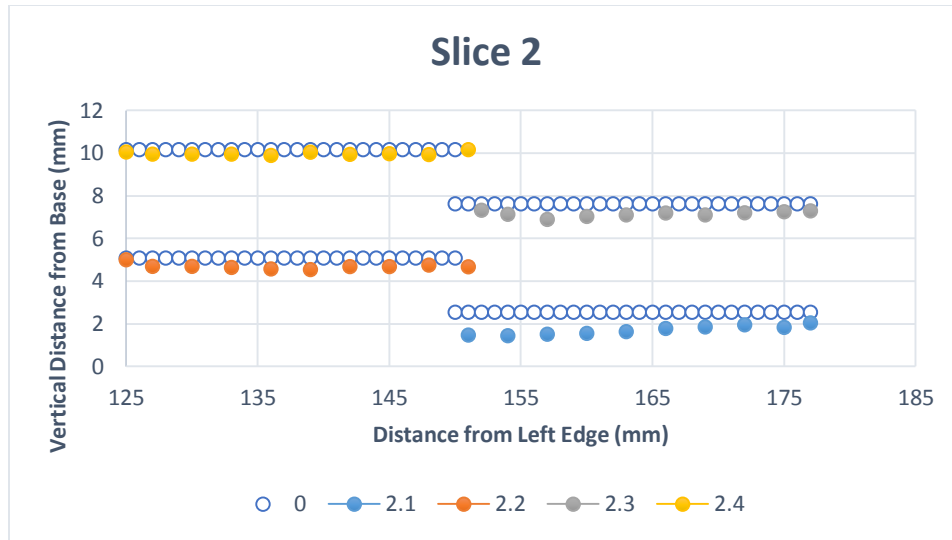


**Figure 47.** Graph of slice 2 of the four layer embedded sample



**Figure 48.** Graph of slice 3 of the four layer embedded sample

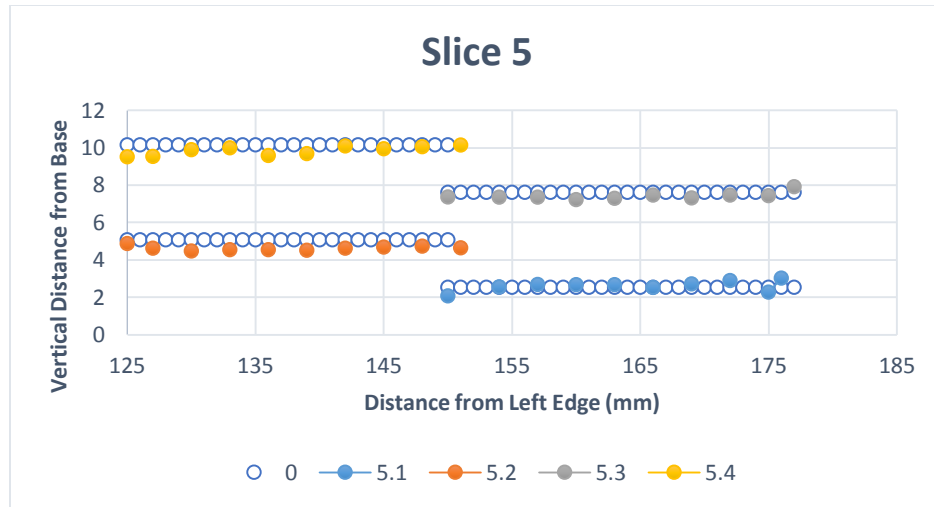


**Figure 49.** Graph of slice 5 of the four layer embedded sample

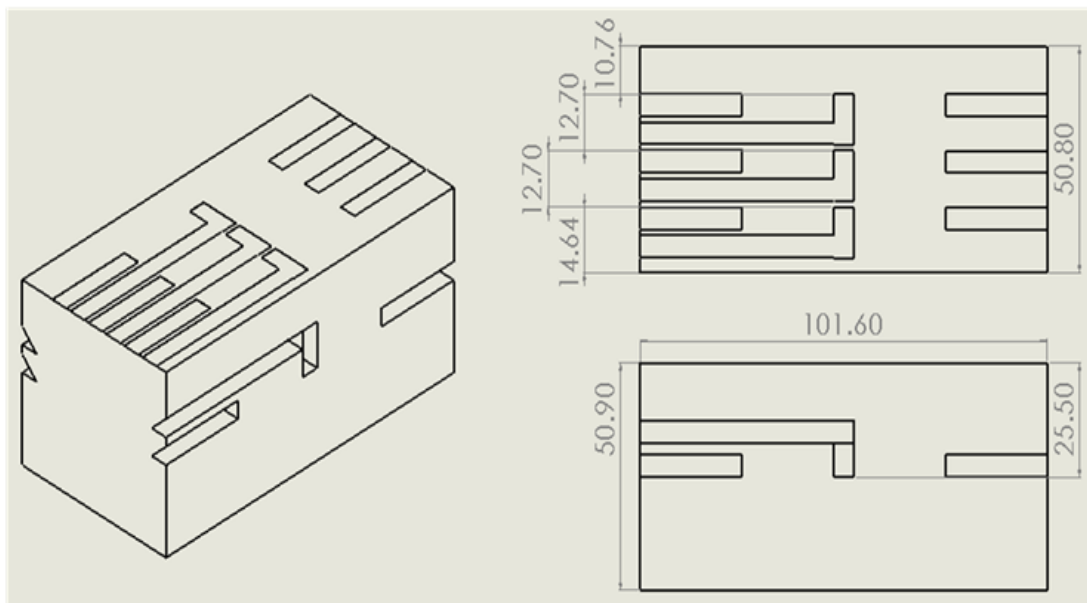


**Figure 50.** Sketch of heat transfer part with dimensions



**Figure 51.** Thermal paste

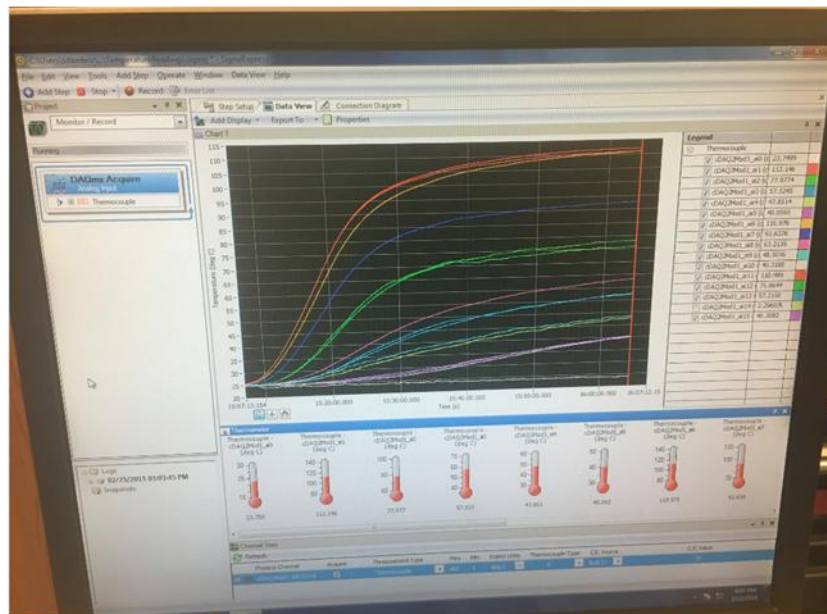


**Figure 52.** Computer generated graph from data collected through the DAQ system

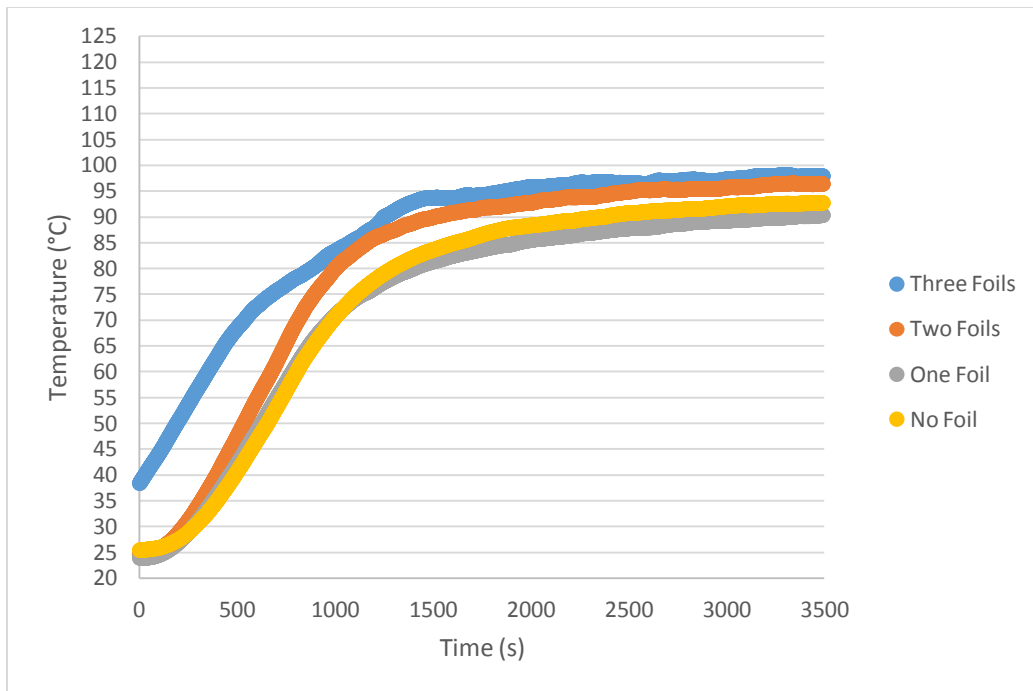


**Figure 53.** Graph of heat transfer at measurement 2

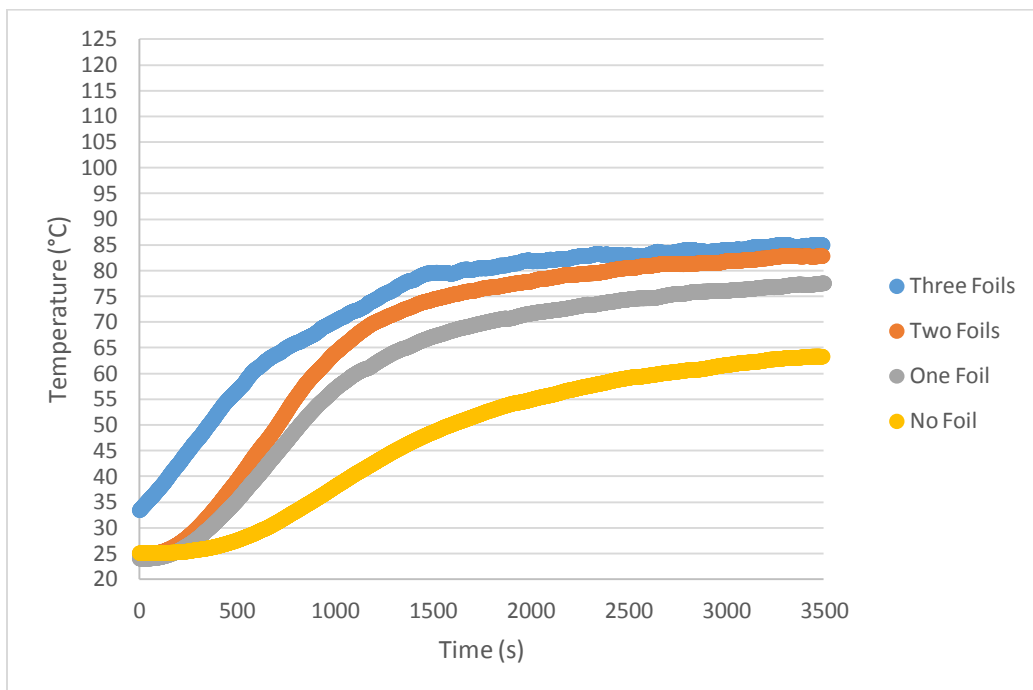


**Figure 54.** Graph of heat transfer at measurement 3

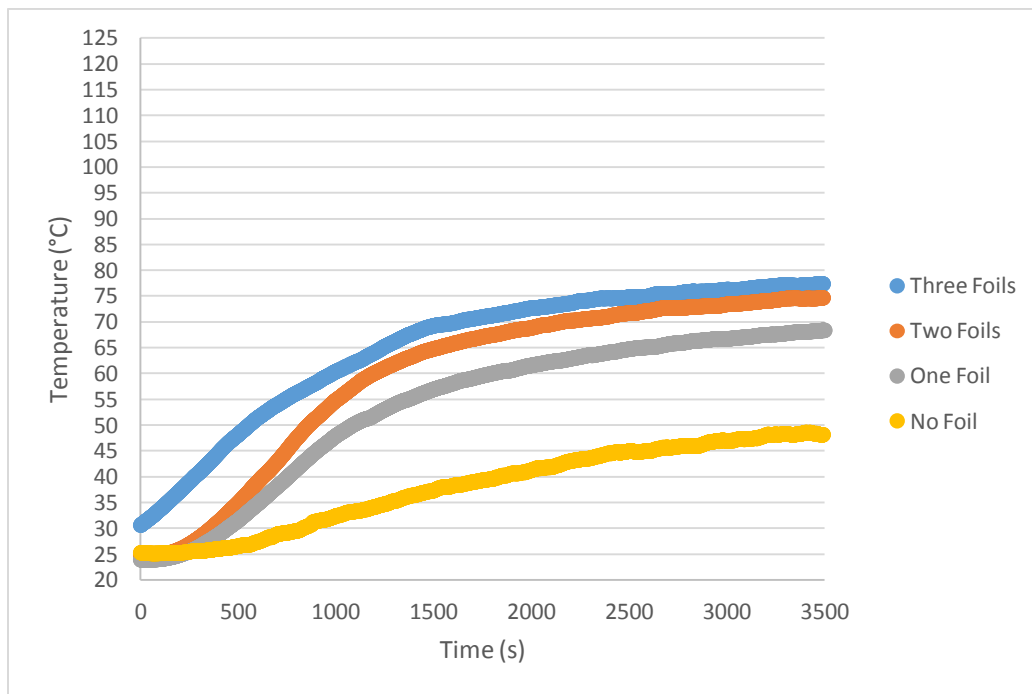


**Figure 55.** Graph of heat transfer at measurement 4



## **CURRICULUM VITA**

Betty Elizabeth McKenzie was born on January 19, 1992 and is the daughter of Mrs. Elizabeth McKenzie and Mr. Michael McKenzie Sr. Betty received her high school diploma in May of 2010 from Clint High School where she was distinguished as a top ten student. She obtained a Bachelor of Science Degree in Mechanical Engineering from the University of Texas at El Paso in May of 2014, the Centennial Graduation. As an undergraduate student Betty was a part of the Marching Miner Regiment, frequently tutored high school students and volunteered every summer to decorate elementary classrooms.

Permanent address: 14608 Pasaje Pl.

El Paso, TX. 79928

This thesis was typed by Betty Elizabeth McKenzie